AD-A065 287 MASSACHUSETTS INST OF TECH LEXINGTON LINCOLN LAB F/G 17/2
CONFIGURATION TRADEOFFS FOR SATELLITE NULLING ARRAYS.(U)
NOV 78 M L BURROWS, J T MAYHAN F19628-78-C-0002
UNCLASSIFIED TN-1978-5 ESD-TR-78-288 NL

1 OF 1
AD
A065287

END
DATE
FILMED
4--79
DDC

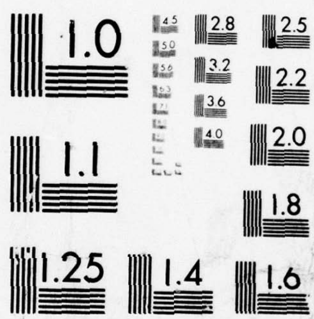
1.0
1.1
1.25
1.4
1.6
1.8
2.0
2.2
2.5
2.8
3.2
3.6
4.0
4.5
5.0
5.6

MASSACHUSETTS INSTITUTE OF TECHNOLOGY

LINCOLN LABORATORY

CONFIGURATION TRADEOFFS FOR SATELLITE NULLING ARRAYS

M. L. BURROWS

Group 64

J. T. MAYHAN

Group 61

TECHNICAL NOTE 1978-5

21 NOVEMBER 1978

LEXINGTON MASSACHUSETTS

ABSTRACT

This paper reviews many of the factors to be considered in deciding upon the relative locations of the elements of an adaptive nulling uplink array antenna on a communications satellite. Discussed are the implications of the limited field of view, the desired resolution, the required coverage away from the null, the weight of the array and its ease of deployment and the resistance to grouped interference sources. Filled arrays, having a performance essentially identical to that of a multiple beam antenna, are described, followed by thinned arrays with their increased resolution but greater vulnerability to grouped interference sources, and hybrid arrays which combine the two array types in an attempt to reduce this vulnerability.

CONTENTS

LIST OF ILLUSTRATIONS

LIST OF ILLUSTRATIONS (continued)

I. INTRODUCTION

Interference suppression by means of antenna arrays in conjunction with adaptive nulling systems has gained much prominence in recent years. To date, most interest has been centered about the adaptive processor following the antenna array, whereas choice of the actual element positioning with the corresponding effect on the nulling performance has received little attention. Consequently, most arrays used consist of a small number of elements spaced at approximately a half wavelength. It is not necessary to accept the limited resolution offered by such a configuration, however, especially in limited-scan applications, and further interesting variations in performance are obtained if the elements are irregularly spaced. While it is generally impossible to determine an optimum array configuration valid for all systems (particularly if mechanical constraints are severe, such as on an aircraft or a satellite), the use of antenna arrays on satellites at geosynchronous orbits poses a special class of problems unique to the narrow field of view (FOV) (i.e., $\pm 9°$ about earth center as viewed from the satellite) and about which useful general statements can be made. It is the purpose of this technical note to discuss some of the technical tradeoffs involved in choosing an array configuration for this application. For simplicity, it is assumed throughout that the bandwidths are narrow enough for monocromatic analysis to be valid. In practical terms, this means that the bandwidth of operation is assumed to be small compared with the reciprocal of the maximum time delay that can occur between the signals received from any two sources in the field of view.

Placing the antenna array elements at spacings of a half wavelength ensures that no spurious grating lobes occur over a very broad field of view. These grating lobes, if not controlled, are undesirable because they can cause an interfering source to appear fictitiously close to a desired user signal direction. However, for the narrow field of view of interest in satellite applications, the inter-element spacing can be increased to as large as 3 or 4 wavelengths while still keeping the grating lobes off the FOV. For this reason, we have found it useful to categorize arrays according to element spacing in the following manner: Filled arrays, having elements located in a regular lattice pattern and, for which, when a maximum directivity beam is scanned to any position on the earth, no grating lobes occur over the remaining FOV. For a satellite at geosynchronous orbit, this corresponds to element spacings on the order of 3-4 wavelengths. Thinned arrays, having almost all elements spaced much greater than 3-4 wavelengths; and finally hybrid arrays, consisting of some combination of a thinned and filled array. Specific examples of such arrays will follow in later sections.

The choice of the particular array which will be used in any final system design will depend on many factors, not the least of which is mechanical deployment of the array in space, as well as the number and locations of nulls, or pattern minima, which must be produced by the antenna. Another factor of considerable importance is the amount of antenna directive gain required to properly close the link between the earth terminal and satellite receiver in the absence of any interference incident on the satellite. Generally speaking, large thinned arrays, properly designed to minimize grating lobes, lead to good nulling resolution on an interfering source, but this good resolution performance must be traded-off against the problem of deploying such an array in space. Smaller numbers of elements lead to less gain and less control of the synthesized patterns away from the null. On the other hand, filled arrays require large numbers of elements for good nulling resolution and hence become more difficult to implement at lower frequencies. An alternate to the filled array is the deployable reflector such as that used with the ATS-6 satellite. In this case, a multiple-beam feed can be used to illuminate the earth FOV, with allowable number of beams (i.e., output ports) increasing with increasing aperture diameter.

Although the use of the multiple-beam antenna (MBA) for adaptive nulling has been discussed elsewhere,[1] and is not the prime interest of this technical note, the concept of packing beams over the FOV is still useful and can be extended to obtain information about the array antenna. In particular, using beam packing considerations, one can estimate the maximum number of output processing ports, K, which it makes sense to use for a given size continuous aperture having diameter D. For $D/\lambda \sim 10$, $K = 7$; for $D/\lambda \sim 16$, $K = 19$;

for $D/\lambda \sim 25$, $K = 37$ and so on, where λ denotes the signal wavelength. Although obtained for an MBA, these results can be extended to the filled array by observing that the array can be converted to an MBA using an orthogonal beam-forming network (BFN). Since the transformation relating the array outputs to the BFN outputs is unitary, the array performance and the MBA performance at a single frequency are identical. It should be noted that, on account of its tapered illumination, a continuous aperture must be somewhat larger than an array aperture to generate the same half-power beamwidth (HPBW). Furthermore, it follows that the HPBW of a thinned array is generally narrower than that of a filled array of the same diameter. For example, we shall show that an equivalent thinned array 5.8 wavelengths in diameter has the same HPBW as a filled aperture of diameter 9.1 wavelengths. The above aperture-size results can then be applied using D_{eq}/λ rather than D/λ, where D_{eq} is the equivalent continuous aperture having the same HPBW as the thinned array. We conclude then that for a satellite antenna operating over the earth FOV, an equivalent continuous aperture diameter of at least 10λ is required to obtain reasonable nulling resolution for an interference source located randomly over the FOV. The HPBW of an aperture any smaller than this would be too large even to pack as small a number as seven beams into the FOV.

II. ALGORITHMS, PATTERN SYNTHESIS AND INTERFERENCE LOCATIONS

Perhaps the most critical facator affecting the number and location of antenna elements is the interference scenario against which the array must operate. A commonly used "rule of thumb" is that an N-element array can produce N-1 independent nulls, and hence the number of elements must increase in proportion to the number of sources to be nulled. However, this conclusion is a very subjective one, and depends to a great extent on the array configuration and separation distance between the interfering sources. Hence, a more precise characterization of the array is desirable, and will now be summarized.

A common way of describing the performance of the array is by way of the covariance matrix $\underline{\underline{R}}$ defined at the array output ports. Denoting the output voltages, normalized with respect to thermal noise, as V_k, k = 1, ...,N, we can then write the general matrix element of $\underline{\underline{R}}$ as

$$R_{k,q} = \langle V_k V_q^* \rangle + \delta_{k,q} \quad , \tag{1}$$

where $\delta_{k,q}$ is the Kronecker delta function, and $\langle\cdot\rangle$ denotes a time average over the interference noise process. The N eigenvalues of $\underline{\underline{R}}$ denote the "degrees of freedom" of the array and a more precise criterion defining the capabilities of the array is that it has N-1 degrees of freedom. If the interference sources are all largely separated, then each degree of freedom corresponds to a single source and the above rule of thumb, associating a single null with each interfering source, is valid. However, if several sources are close together, then they might engage only one or two degrees of freedom, depending on the array configuration. The problem here is defining how close is "close". We shall show later that for the filled array or thinned array, "close" implies less than a single HPBW of the total array uniformly excited. However, for the hybrid array, "close" depends strongly on the number of interference sources, as the algorithm controlling the operation of the array can then "turn off" selected elements to control the degrees of freedom used by the array. This leads us to define the following three classes of interference scenarios used to evaluate the performance of particular arrays: Separated (relative to HPBW) point sources; distributed, but localized group sources (i.e., many sources within a single HPBW); and combinations of these two, separated plus group sources, all assumed to be equally probable anywhere over the FOV.

There are many algorithms which have been proposed for control of adaptive processors, and since it is not the purpose of this technical note to discuss these as such, we assume the adaptive weights $\underline{w}$ are set according to the most common technique[2]:

$$\underline{w} = [\underline{\underline{I}} + \mu \underline{\underline{R}}]^{-1} \cdot \underline{V} \quad , \tag{2}$$

where μ represents the effective gain of the adaptive processor, $\underline{V}$ is a "beam steering" vector and $\underline{w}$ the adapted weight. The beam steering vector $\underline{V}$ controls the mode of operation of the array (i.e., the quiescent radiation pattern) in the absence of interference. For satellite systems employing FDMA, where many randomly located user signals are simultaneously being processed, a convenient mode of operation is earth coverage. For the array, assuming an individual element has enough gain, this might correspond to a steering vector $\underline{V} = \text{col}\ [0,\ldots 0,\ 1,\ 0,\ldots 0]$, i.e., earth coverage is obtained by simply exciting a single element. The other elements are then used as needed in conjunction with the EC reference to minimize the interference in the output of the array.

For simplicity, all user signals are assumed to be less than the system thermal noise level as might well occur for a system employing spread sprectrum techniques in conjunction with adaptive nulling. The sensitivity of array performance to choice of EC reference element is deferred to a later section.

In the following three sections, we will discuss the relative merits of each of the three classes of arrays introduced in Section I. We begin with the most straightforward class, the filled array.

III. A CLASS OF FILLED ARRAYS FOR SATELLITE ANTENNA NULLING

From a mechanical deployment viewpoint, the degree to which one can fill an aperture is strongly dependent on the frequency band of operation of the antenna system. For example, at X-band, operating at 8.15 MHz, a multiple-beam lens having an aperture diameter on the order of 30λ (1.14m) and employing 61 beams to illuminate the earth FOV is already in the design stage.[3] On the other hand, at UHF, where the wavelength is some 30 times larger, achieving aperture diameters of this magnitude is more difficult. One alternative to the deployable reflector mentioned in Section I is to deploy an array with elements spaced 3-4λ (eliminating grating lobes over the FOV) having less maximum directive gain than the lens or reflector, but essentially the same radiation pattern characteristics (e.g., HPBW, sidelobe levels, etc). The purpose of this section is to develop the array parameters best approximating the radiation pattern characteristics of a continuous circular aperture of diameter D. To this end, it is convenient to choose an array configuration in the form of a regular hexagonal lattice, with an array element at each lattice point. From our point of view, this is desirable in the sense that the regular periodicity of the lattice leads to the realizability of a beam-forming network which can be used to obtain the various preprocessing advantages peculiar to an MBA,[1] if desired. We note that because of the lattice symmetry, all the degrees of freedom of the array might not be fully exploited against particular interference sources placed to take advantage of this symmetry. Hence, for a small number of elements, such an array would probably not be used, since a thinned array would yield better performance. As the number of elements increases, however, this effect disappears and a meaningful array configuration can be generated.

Before considering the general case, we digress briefly and consider the one-dimensional characterization of a linear aperture by a <u>uniformly spaced</u> array. Trends indicated using this simpler geometry illustrate the basic tradeoffs between the filled array and the continuous aperture.

A. <u>Linear Apertures and Linear Arrays</u>. Consider the linear aperture of length D illustrated in Fig. 1. The radiation pattern for uniform illumination of the aperture is given by

$$E(\theta) = \frac{\sin(\frac{kD}{2}\sin\theta)}{(\frac{kD}{2}\sin\theta)} \quad , \tag{3}$$

where θ is the angle measured from broadside and $k = 2\pi/\lambda$. This pattern has the following characteristics:

$$\begin{aligned} &\text{HPBW} \sim .88\ \lambda/D \\ &\theta_N = \sin^{-1}(\lambda/D) \\ &\theta_{SL} = \sin^{-1}(1.5\ \lambda/D) \quad , \end{aligned} \tag{4}$$

where HPBW = half-power beamwidth, θ_N = first null position and θ_{SL} = first sidelobe position. The first sidelobe level is 13 dB below the main-beam peak.

If we now consider a two-element array with elements positioned at each end of the aperture, then the radiation pattern takes the form

$$E_2(\theta) = \cos\left(\frac{kD}{2}\sin\theta\right) \quad . \tag{5}$$

In this case, each lobe of the pattern constitutes a grating lobe. The appropriate parameters are

$$\begin{aligned} &\text{HPBW} \sim .5\ \lambda/D \\ &\theta_N = \sin^{-1}(.5\ \lambda/D) \\ &\theta_{GL} = \sin^{-1}(\lambda/D) \quad . \end{aligned} \tag{6}$$

Note in particular that HPBW and θ_N have decreased considerably from those for the filled aperture of diameter D, confirming the proposition that the

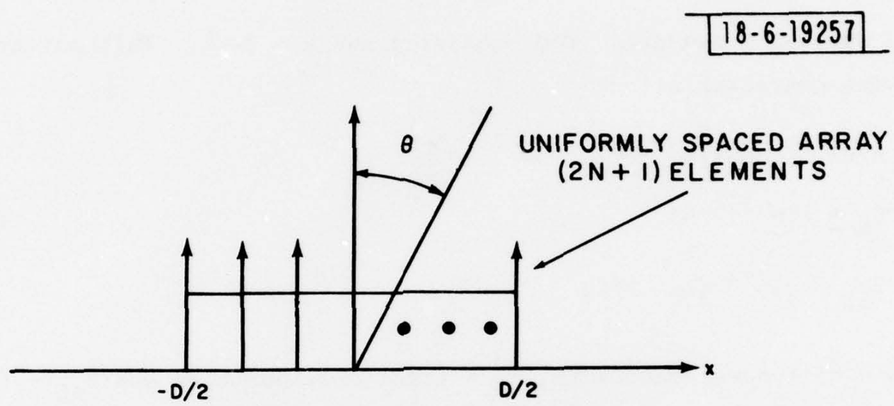

Fig. 1. Approximating a linear aperture with an array.

two-element array is equivalent in resolution to a somewhat larger filled aperture.

Next, consider 2N+1 regular spaced elements filling the aperture. In this case

$$E_{2N+1}(\theta) = \frac{1}{2N+1} \frac{\sin(\frac{2N+1}{2N} \frac{kD}{2} \sin\theta)}{\sin(\frac{1}{2N} (\frac{kD}{2}) \sin\theta)} \quad . \tag{7}$$

The appropriate parameters characterizing the pattern become

$$\theta_N = \sin^{-1} (\frac{2N}{2N+1} \frac{\lambda}{D})$$

$$\theta_{SL} = \sin^{-1}(\frac{3N}{2N+1} \frac{\lambda}{D}) \tag{8}$$

$$\theta_{GL} = \sin^{-1}(2N \frac{\lambda}{D}) \quad .$$

Observe that as N increases, the grating lobe moves out and the pattern approaches that of the uniformly illuminated aperture, Eq. (3). In particular, note that for N = 2 (5 elements), θ_{GL} has moved out to approximately 4 times λ/D. For a HPBW of 7° (which needs, at UHF, a continuous-aperture diameter of about 9 m), the grating lobe is well outside the FOV. From (3) and (7), we see that the regular linear array of aperture D' has the same values of HPBW and θ_N as a continuous linear aperture of length D if

$$D' = \frac{2N}{2N+1} D \quad . \tag{9}$$

For N=1 (3 elements), a 33% decrease in aperture is obtainable. For N=2 (5 elements), a 20% decrease results. Of course, the position of the grating lobe must be checked to assure it lies outside the FOV. The general trend is clear however; when operating over a fixed FOV, generally one can employ an array over a smaller diameter to approximate the radiation pattern characteristics of a larger continuous aperture. These effects will now be quantified for three types of planar arrays.

B. A Simple Class of Planar Arrays. Equi-spacing a set of array elements over a given planar surface is readily accomplished using a hexagonal lattice structure, similar to the lattice used in packing a set of circular beams to illuminate the earth FOV. The hexagonal lattice has the property that each point is equi-distant from all six of its nearest neighbors via the sides of an equi-lateral triangle. This particular lattice structure has also found application in phased arrays, for which it eases the problem of grating lobes caused by periodic array spacing. In the following, we consider the class of hexagonal array geometries illustrated in Fig. 2. The 13-element geometry is considered as a simple extension of the seven-element geometry since it employs the same number of mechanical "booms" which would emanate from the satellite body. The outermost elements, however, are equi-spaced only from their neighbors on the same arm. The aperture D' for the array best approximating a continuous aperture of diameter D follows the same tradeoffs discussed above for the linear aperture; namely, a tradeoff exists between half-power beamwidth HPBW and first null position θ_N on the one hand, and the location of the grating lobes in the field of view, on the other. Generally speaking, if one uses a beam-forming network to steer a beam to the edge of the earth, the grating lobe must be kept at least 20-25 degrees from the peak of the outer beams in order to remain outside the FOV. This constraint limits the maximum diameter one can use with the array. On the other hand, using too small a diameter leads to a broader beam, because HPBW increases with decreasing diameter, resulting in less nulling resolution. Thus, for each array geometry, a compromise must be made in the choice of HPBW and θ_{GL}. The sidelobe levels, however, are a function only of the symmetry of the array; i.e., only their relative positions change as the diameter changes. The sidelobe level is important in obtaining good spatial discrimination from beam-port to beam-port if the array is to be used in conjunction with an MBA.

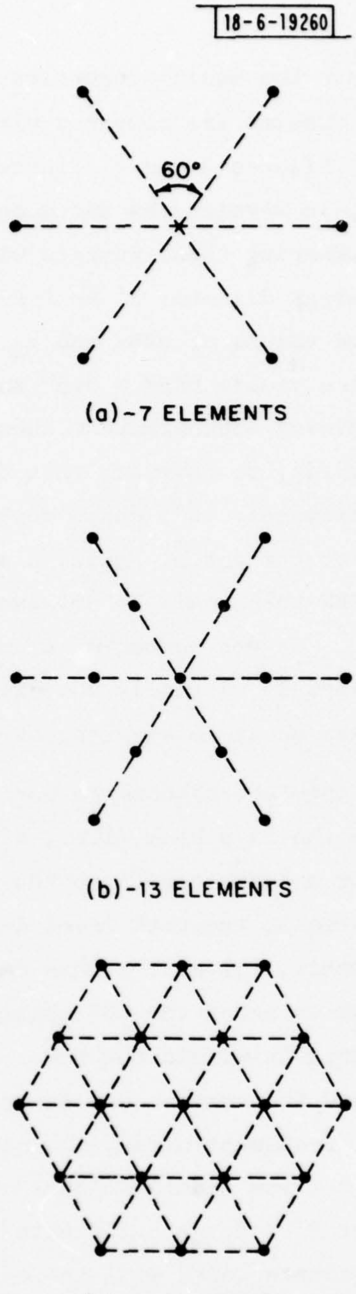

Fig. 2. A class of regularly spaced hexagonal arrays.

Figures 3 to 6 illustrate the basic properties of each of the array configurations of Fig. 2. The results are compared with those of a continuous aperture where appropriate. Figures 3 and 4 illustrate the HPBW and first null positions vs array diameter, in wavelengths and meters (at 350 MHz), for each of the array geometries. Comparing these results with those for a continuous aperture, we note that the array diameter D' is less than the continuous-aperture diameter D for fixed values of HPBW and θ_N. For example, a 10.5-wavelength continuous aperture yields HPBW $\sim$ 5.5° and θ_N = 7°. The diameter D' for the 7-element array giving approximately these same values would be about 8 wavelengths. We note from Fig. 5, however, that for this value of D', the grating lobe occurs at approximately 16°, which would be in the FOV for a beam displaced to the outer edge of the earth. Hence a smaller diameter should be used, compromising on the HPBW that could be obtained with a continuous aperture 10.5 wavelengths in diameter. As the number of elements increases this compromise is less severe, and indeed is virtually non-existent for the 19-element array if D' is no greater than about 16 wavelengths.

To illustrate this grating-lobe phenomenon more clearly, we plot in Fig. 6 the peak power level outside the main beam (i.e., either sidelobe or grating lobe) over the entire FOV for a beam steered to the outer edge of the FOV. For the 7-element array, and D' small, the peak level is the nominal sidelobe level determined by the array geometry, -11 dB for this case. As D' increases, the grating lobe gradually begins to enter the FOV until finally, for $D'/\lambda \gtrsim 10.5$, the entire grating lobe maximum is within the FOV. Note however, that the grating lobe is very localized in position and exists over only a small fraction of the earth. For the 19-element array, the pattern behavior is much better. Note in particular the low sidelobe level of -15 dB out to diameters as large as 15λ. Noting that D' < D, we anticipate from this result that the 19-element array would approximate quite well the radiation pattern characteristics of a continuous aperture of $D/\lambda = 16$. The behavior of the 13-element array geometry is similar to the other two, except that for $D'/\lambda \lesssim 9$, the first sidelobe peak does not occur within the FOV for a beam shifted to the edge of the FOV. Thus, for D" small, and as D" increases, the sidelobe gradually enters

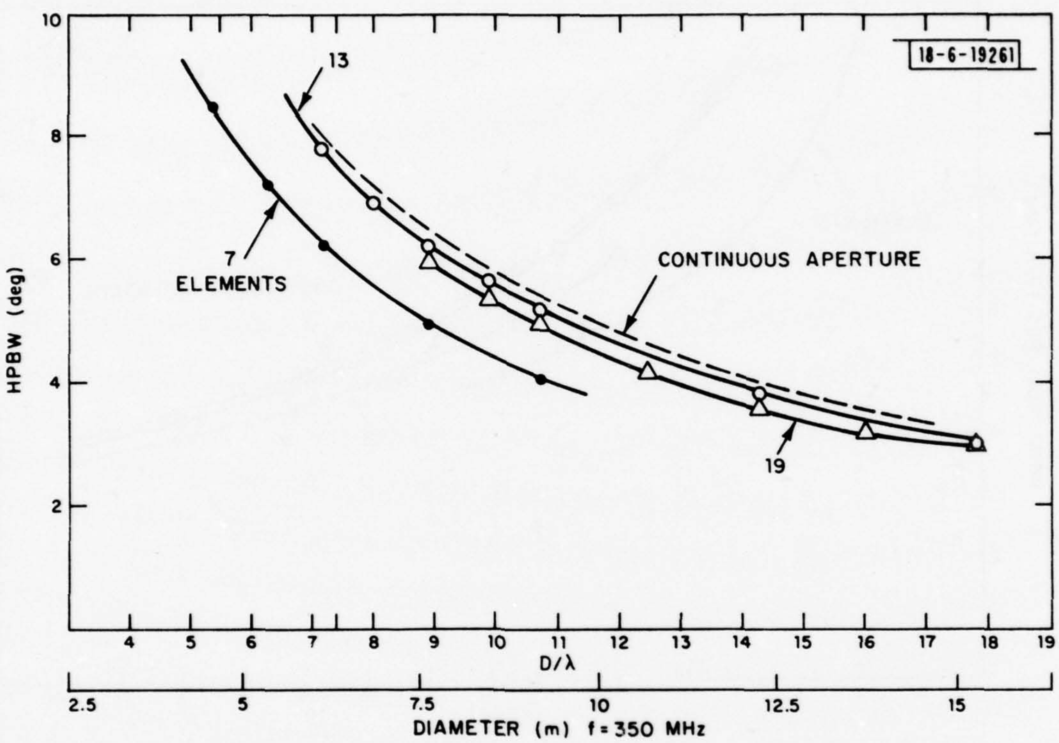

Fig. 3. Half-power beamwidth for the class of hexagonal arrays in Fig. 2 vs D/λ, or D at f_o = 350 MHz.

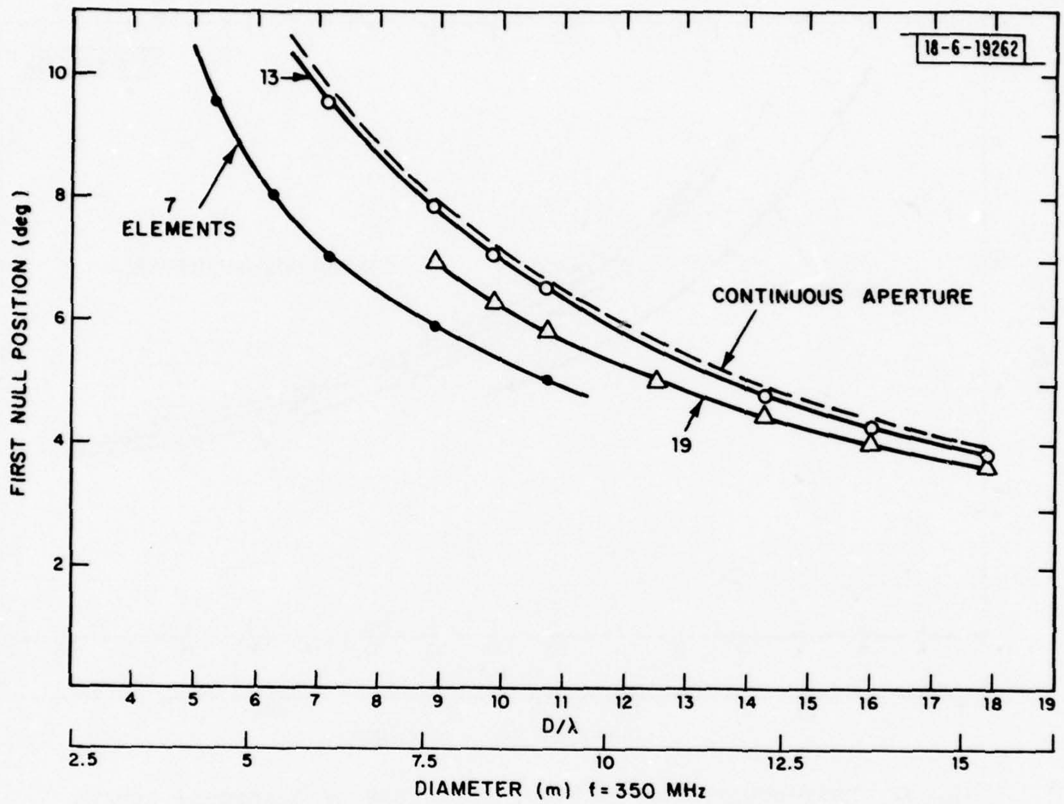

Fig. 4. First null position vs D/λ for the class of hexagonal arrays of Fig. 2.

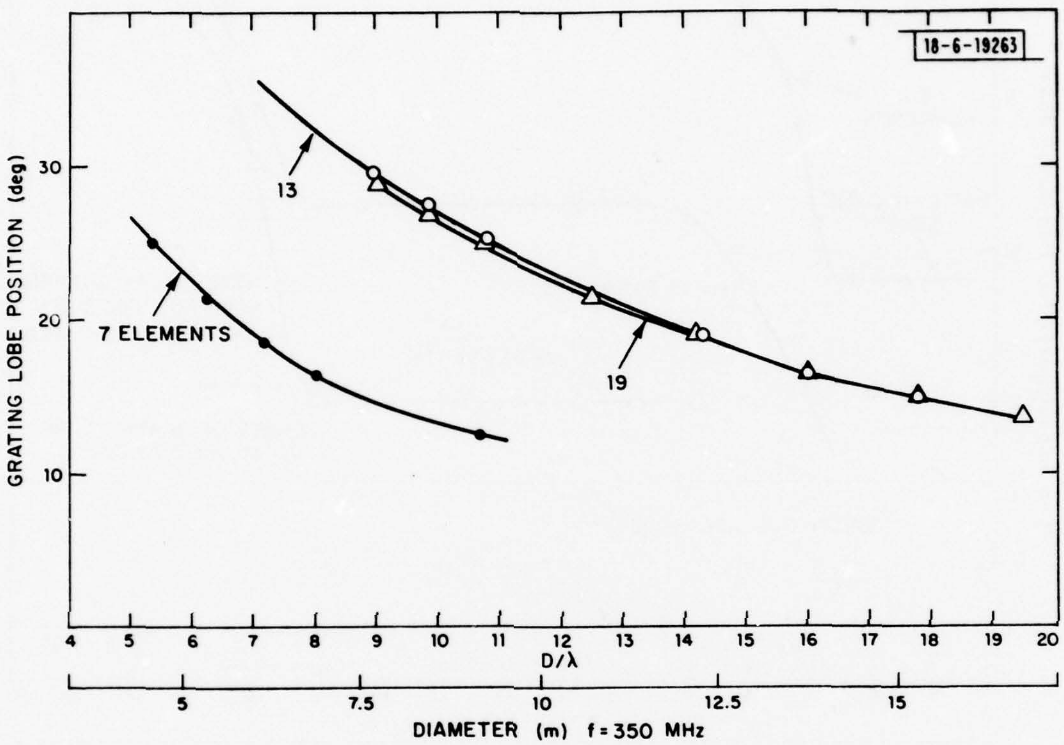

Fig. 5. Grating lobe position vs D/λ for the class of hexagonal arrays of Fig. 2.

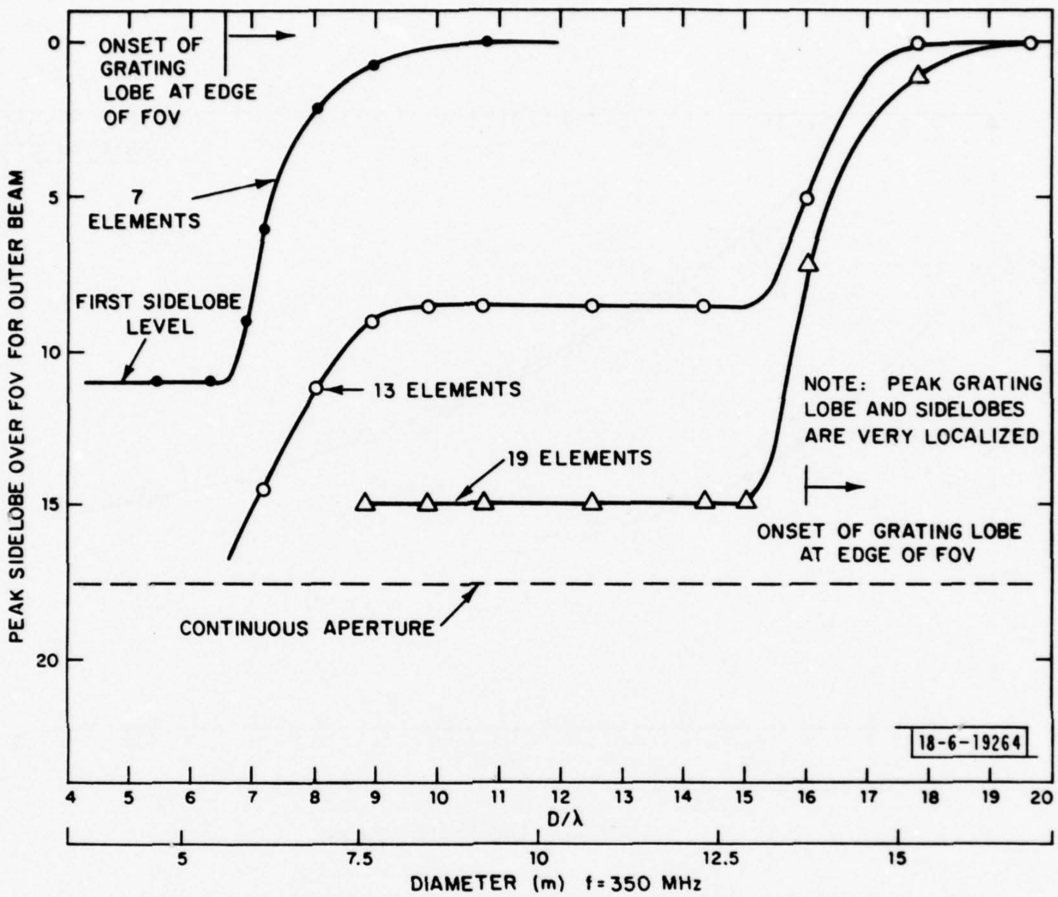

Fig. 6. Peak sidelobe level over the FOV for the class of hexagonal arrays of Fig. 2.

the FOV as indicated in the figure. The sidelobe level of -8.5 dB is higher than the value of -11 dB for the 7-element array, indicating the lack of complete hexagonal symmetry.

C. Some Example Radiation Patterns. Figures 7 to 9 illustrate the broadside radiation pattern for each of the arrays of Fig. 2 when approximating the performance of the 10.5λ filled aperture over a ±16° angular grid. The beam located at (0,0) on the grid can be viewed either as a beam illuminating the center of the FOV or as a beam displaced to the edge of the FOV. The latter case is indicated in the figures where the outline of the earth FOV (angular radius 8.5°) is encircled on the figure. Observe that for the 7-element array, the grating lobe just starts to enter the FOV. For the 13-element array, the grating lobe is far removed from the FOV, but the sidelobe level of -8.5 dB is present in three localized positions over the FOV. Finally, the 19-element pattern shown in Fig. 9 illustrates the excellent behavior of this array in approximating the performance of the 10.5λ continuous aperture. The corresponding 19-element approximation to a 16λ continuous aperture is illustrated in Fig. 10 using D' = 14.3λ. Observe that the sidelobes are low everywhere over the FOV for the beam at the edge of the FOV, and the grating lobe is just removed from the earth FOV. It should be noted, however, that although the angular properties of the continuous aperture radiation pattern have been approximated quite well, the directive gain available from the array is less. For the beam patterns illustrated in Figs. 7 to 10, we have used the gain expression

$$G \approx NG_o \quad , \tag{10}$$

where G_o is the element gain. For example, if each element consists of four crossed dipoles over a ground plane $G_o \approx 13$ dB. The maximum directive gain obtainable for the thinned array vs the filled aperture is compared in the following table. Note that the main drawback of the array compared to the filled aperture is the reduction in absolute directive gain. At UHF, however, link calculations show that many eminently useful communication possibilities

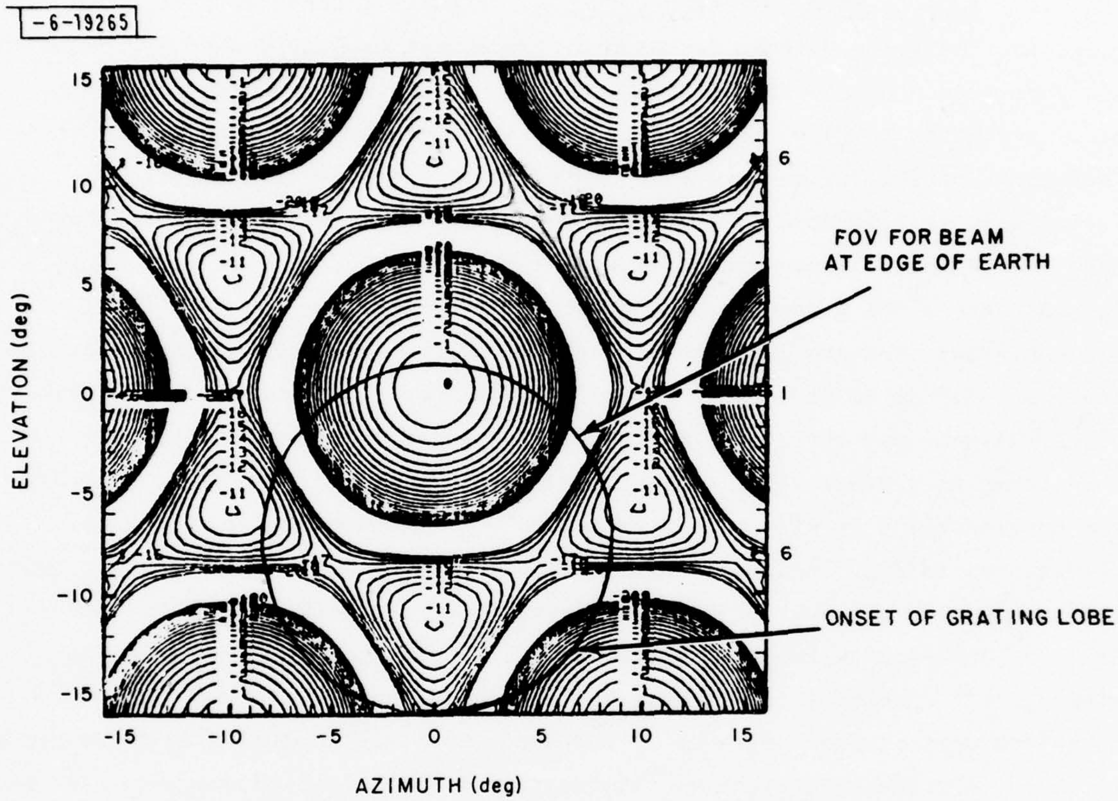

Fig. 7. Maximum directivity beam over the FOV for the seven-element hexagonal array (D'/λ = 6.8).

-6-19266

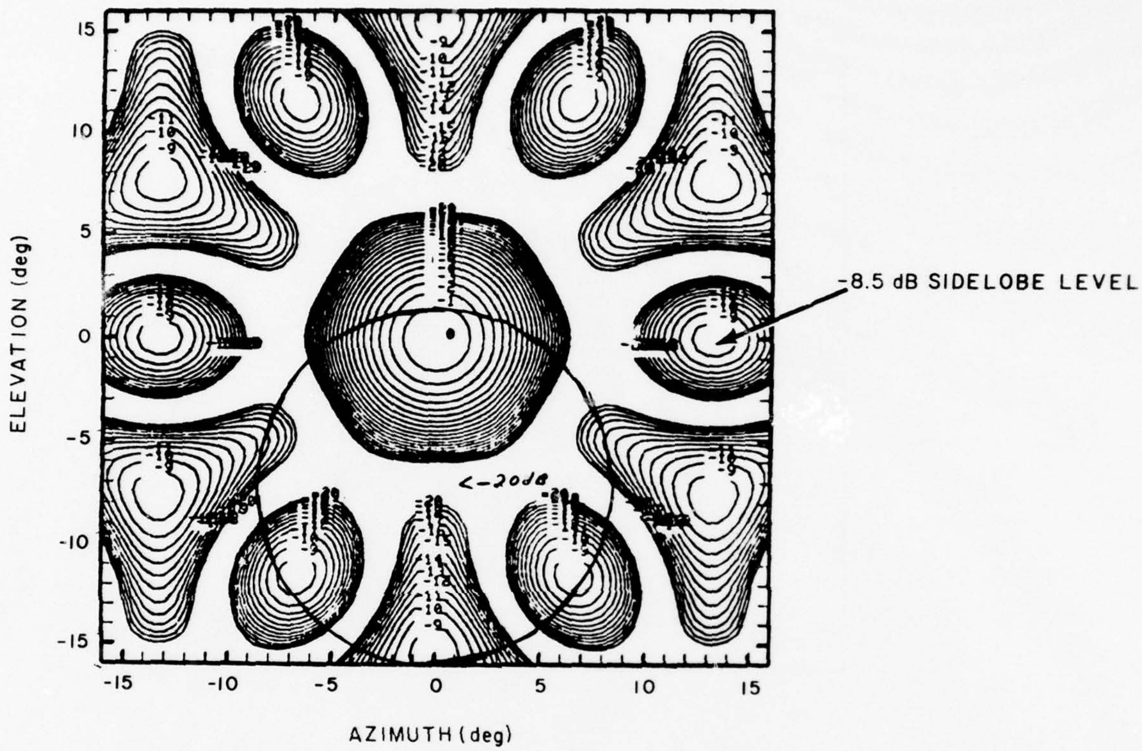

Fig. 8. Maximum directivity beam over the FOV for the 13-element hexagonal array ($D'/\lambda = 10$).

-6-19267

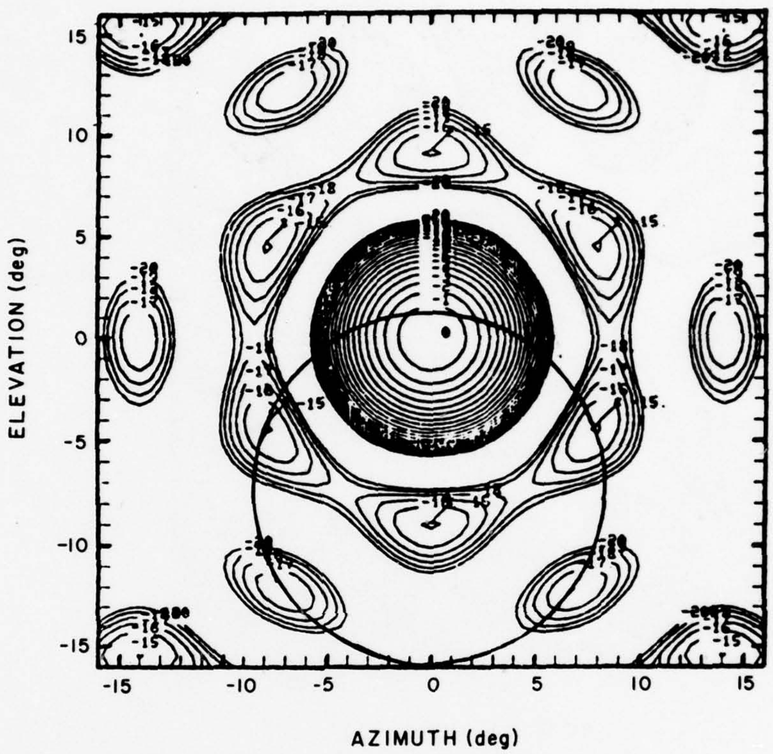

Fig. 9. Maximum directivity beam over the FOV for the 19-element hexagonal array ($D'/\lambda = 9.5$).

– 6-19268

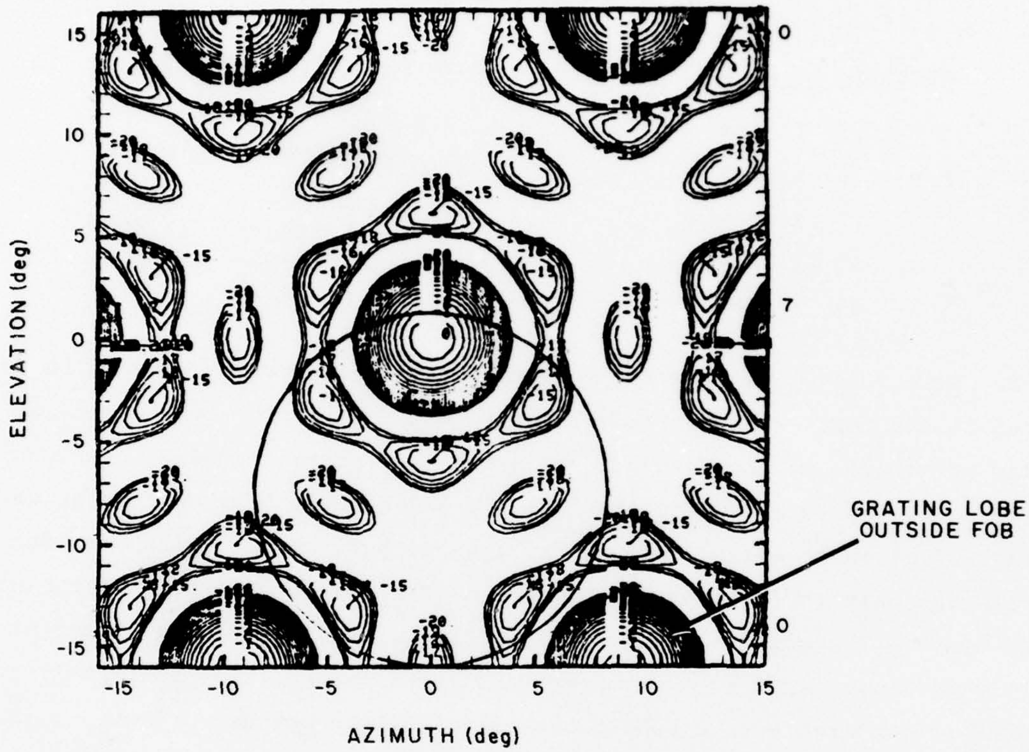

Fig. 10. Maximum directivity beam over the FOV for the 19-element hexagonal array ($D'/\lambda = 14.3$).

exist even with this reduction.

TABLE II

BEAM PEAK DIRECTIVE GAIN FOR PARTIALLY-FILLED ARRAY AND FILLED APERTURE

Aperture or Array	Beam Peak Directive Gain	
D = 10.5λ filled	27.5 dB	(50% efficiency)
D = 16λ filled	31.0 dB	
7 Elements	21.5 dB	(assuming 13 dB element gain)
13 Elements	24.1 dB	
19 Elements	25.8 dB	

D. Some Nulling Results for a 19-Element Filled Array. As will be demonstrated in the next section, the nulling resolution of some of the smaller regular arrays discussed above can be improved by array thinning, or by using the smaller array as a "sub-cluster" (e.g., a 7-element hexagonal array with "outrigger" elements added). Thus, for example purposes, we will consider in this section only the nulling performance of the 19-element filled array discussed above. The array elements are positioned hexagonally, and comprise an aperture 14.3 wavelengths in diameter. Element spacing is approximately 3.5λ. The HPBW is comparable to a continuous 16λ diameter aperture. The 19 degrees of freedom plus full aperture control assure a reliability against most interference threats except one uniformly spread out over the total FOV. To illustrate this, we assume an adaptive processor having a 40 dB dynamic range (i.e., $\mu S_{max} = 10^4$, where S_{max} is the maximum eigenvalue of R), and consider each class of interference scenarios categorized in Section II. First, a single large ($\mu S_1 = 10^4$) interference source is located as shown in Fig. 11, where we have illustrated the radiation pattern with a null (all contour values are in dBi) placed on the interference. The steering vector $\underline{V}$ was chosen to be that of earth coverage; i.e., $\underline{V}$ = col [1, 0, ..., 0], which corresponds to excitation of the center array element alone. Each coverage gain is thus 13 dB and is approximated well over the majority of the FOV. The resolution obtained on the

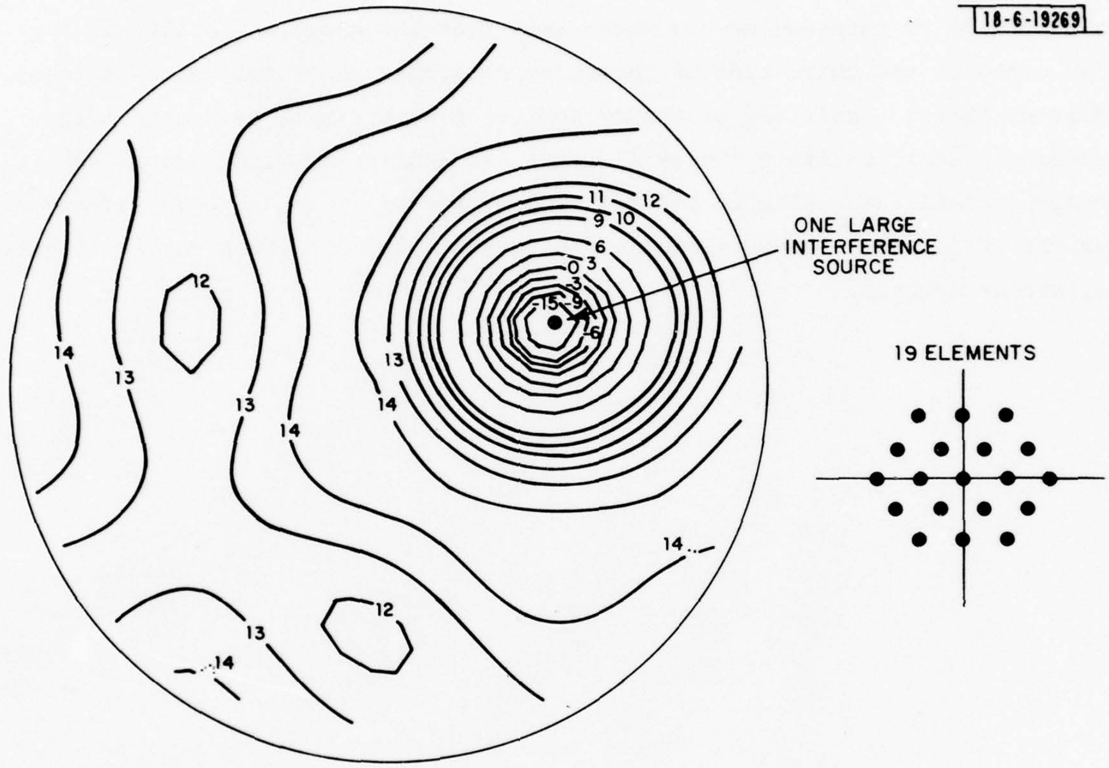

Fig. 11. Radiation pattern of 19-element hexagonal array with null on single large interference source ($D'/\lambda = 14.3$).

interference source is consistent with that of a 16-λ continuous aperture. In Fig. 12, we consider a localized group interference threat consisting of ten weak sources ($\mu S_1 \approx 10$ for each individual source) located in the same geographic area. Note that a broad null has been formed on the group, and earth coverage gain of >13 dB is obtained as one moves away from the group. Finally, in Fig. 13, we consider the third type of interference scenarios of interest: a localized group threat consisting of weaker sources plus a single separated large interference source. Since the 19 elements are consistent with a total FOV coverage (recall the analog to the MBA, where, for $D/\lambda \sim 16$, 19 beams adequately cover the entire FOV), good resolution is obtained both on the group and isolated interference sources.

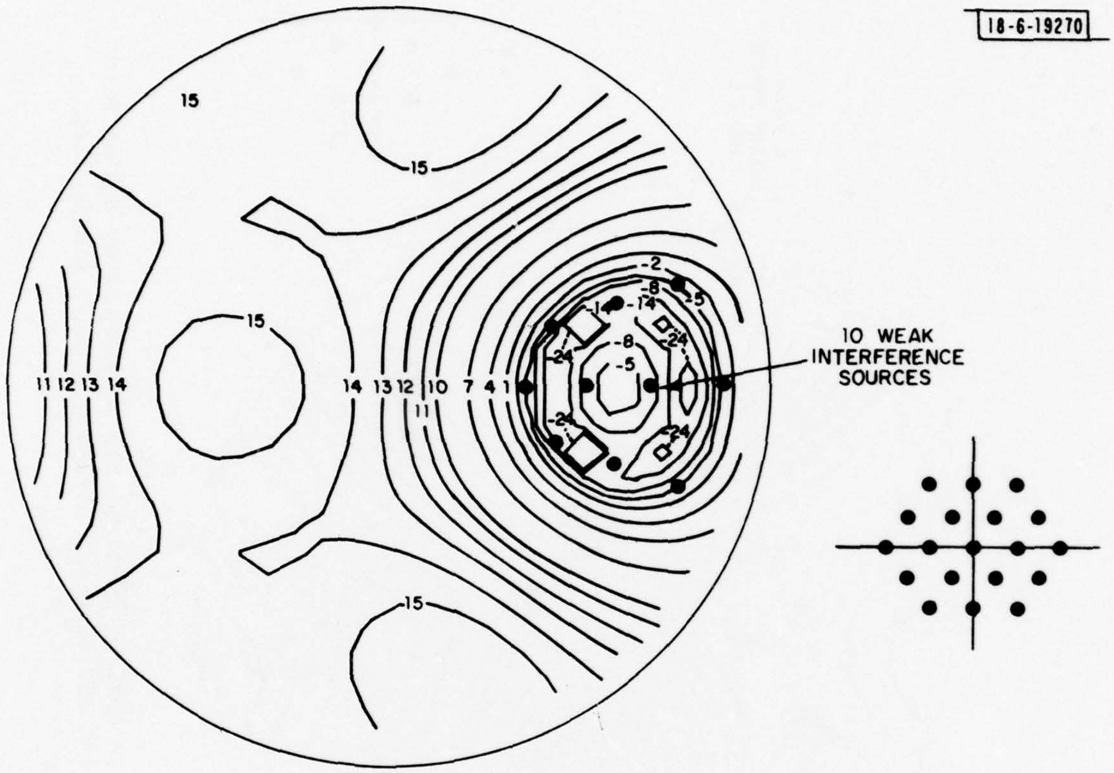

Fig. 12. Radiation pattern of 19-element hexagonal array having broad null on a localized group interference scenario (D'/λ = 14.3).

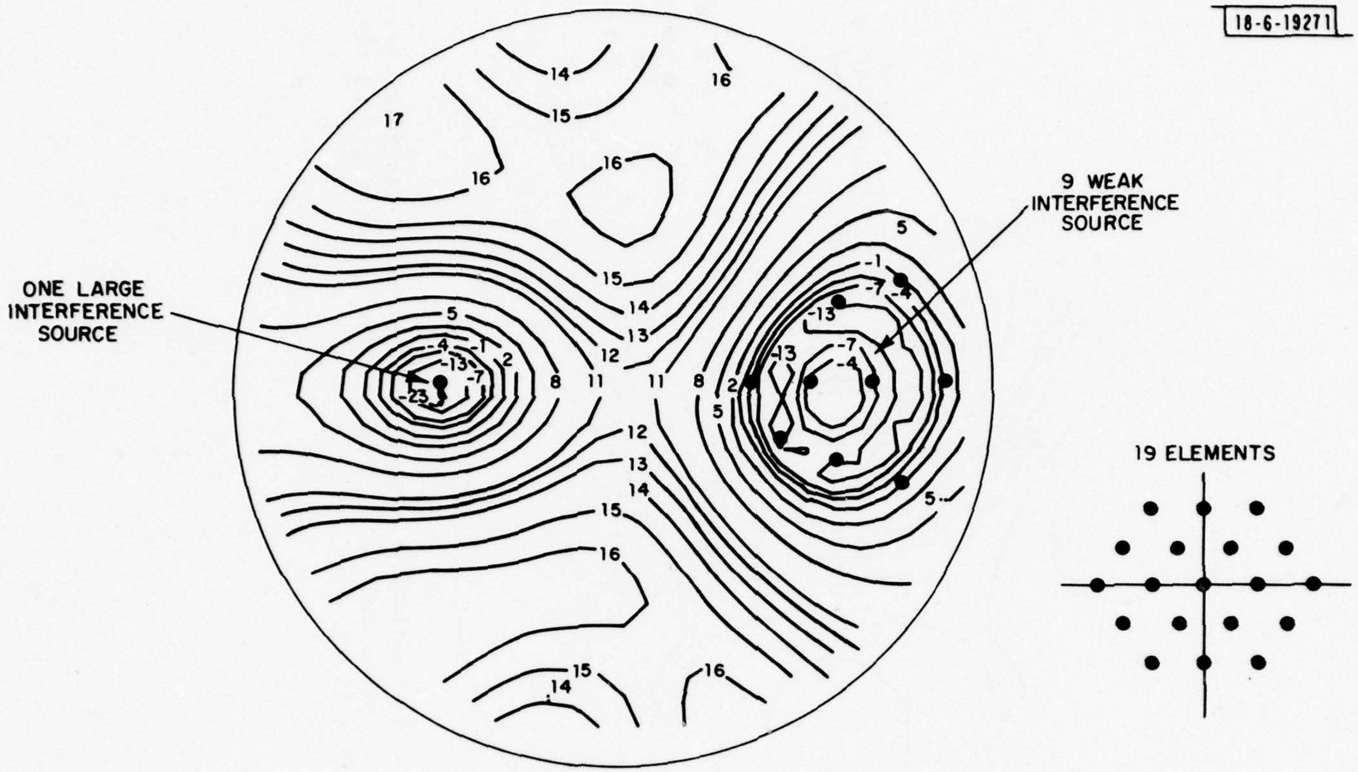

Fig. 13. Radiation pattern of 19-element hexagonal array having broad null on distributed interference and narrow null on a single large interfering source ($D'/\lambda = 14.3$).

IV. THINNED AND HYBRID ARRAYS

A. Introduction. In its simplest terms, the case for thinning is that the resolution of the array is good if the maximum element spacing is large and that grating-lobe problems are avoided if the minimum element spacing is small enough. Fewer elements are required to achieve these properties if the array is thinned than if it is filled. For example, a linear array having a maximum element spacing ten times the minimum spacing needs a minimum of only three elements, if it is thinned, whereas a filled array would need eleven. The corresponding numbers for a plane array are, perhaps, five and as many as a hundred, respectively. Thus, a large reduction in the number of elements and weight controls can be obtained by thinning the array.

Other considerations, however, intervene to prevent the difference between the numbers of elements from being so extreme in practice. One is the need to provide sufficient gain for communication in the user direction. If the number of elements is too small, the gain patterns of the array after nulling can be very uneven, leading to unacceptably low gain in some user directions. Another consideration is the number of interference sources likely to be encountered. To be sure of being able to point nulls in the direction of J different interference sources, we require J+1 separately weighted antenna elements.

One important further consideration which tends to increase the number of elements of a thinned array is the need to avoid making it vulnerable to the grouped interference threat described earlier. The problem arises because the solid angle Ω_c enclosed by one resolution cell of a thinned array is much less than Ω_o/N, where Ω_o is the solid angle enclosed by the whole field of view and N is the number of elements. For a filled array, Ω_c is essentially equal to Ω_o/N. A set of N interfering sources, if they are to overload all the available degrees of freedom of the nulling antenna system, must be separated from their nearest neighbors by at least the width of a resolution cell. For the filled array, therefore, the sources must be spread more or less uniformly over the whole field of view, but for the thinned array, they can be grouped in a much smaller region. Thus, a group of interference sources located in a single small region of the field of view can effectively jam communication traffic from anywhere in the whole field of view, if the array is thinned but improperly designed. One solution to this grouped-source vulnerability of thinned arrays is to ensure that among the complete set of thinned-array elements there exists a subset of elements separately capable of pointing a broad null in the direction of the jammer group. Thus, one obtains a hybrid array having a rudimentary filled subarray as part of the whole thinned array. It has more elements than a purely thinned array, but far fewer than does a filled array of the same overall aperture.

Once the desirability of thinning an array has been decided, the question of the exact placement of the elements arises. At present, there exists no general theoretical approach to the problem of configuration optimization. This is because, in the first place, it is difficult to define the performance criteria for the array, and second, that the number of parameters to be jointly optimized is so large. Thus, the complexity of the problem has made it impossible so far to devise an algorithm which would define the element locations, optimized to any reasonable criteria, and, moreover, a practical criterion has yet to be constructed.

These difficulties make it necessary to fall back on trial and error for determining the element locations, and using subjective judgement to combine the various piecemeal measures of array performance into an overall ranking. Thus resolution, gain coverage and null depth on grouped jammers are separate measures of array performance whose relative importance depends upon the situation being considered.

One further point which needs to be made on the choice of the element locations concerns the mechanical constraints. In practice, the range of possible configurations is strongly limited by the length, weight, number and disposition of each element together with its deployment boom. This means that even if the ideal electrical configuration could be identified, it might well be incompatible with the mechanical constraints. In practice, therefore, the final element locations are reached by a process of interactive evolution, trading off the electrical and mechanical properties.

The next two Sections present some data on the performance of various example arrays which illustrate the principles described above. The third and fourth Sections are brief discussions of the effect of physical symmetry and electrical symmetry, respectively, on the performance of the array.

B. The Resolution of Thinned Arrays. Figure 14 is a contour plot of the directive-gain pattern of the seven-element regularly spaced hexagonal array, described in Section II, showing a null formed in the direction of an interference source. A single-element earth-coverage beam steering weight is used. The large circle indicates the limb of the earth as seen from synchronous altitude. As discussed in Section II, the array is a regular filled array having an element spacing as large as possible while still preventing the grating nulls from intruding onto the field of view. The presence of a grating-null lying off the top right-hand corner of the plot is clearly indicated, showing that the skirts of this null are apparent in the field of view even though the center of the null is outside it.

The resolution of the array, using for convenience the 0-dB contour as a guide, is some 5.5°. The resolution can be substantially increased by increasing the size of the array, as Fig. 15 shows, but then the field of view becomes riddled with grating nulls.

The pattern of a thinned array which avoids the grating null problem is illustrated in Fig. 16. It does so by breaking up the simple regularity of the large hexagonal array. The array consists of the two concentric square arrays shown, each of which, by itself, would produce a directive-gain pattern in the form of a square cellular lattice having a cell size inversely proportional to the size of the square array. The two lattices are inclined at 45° from one another. The conditions under which the sensitivities of the two square

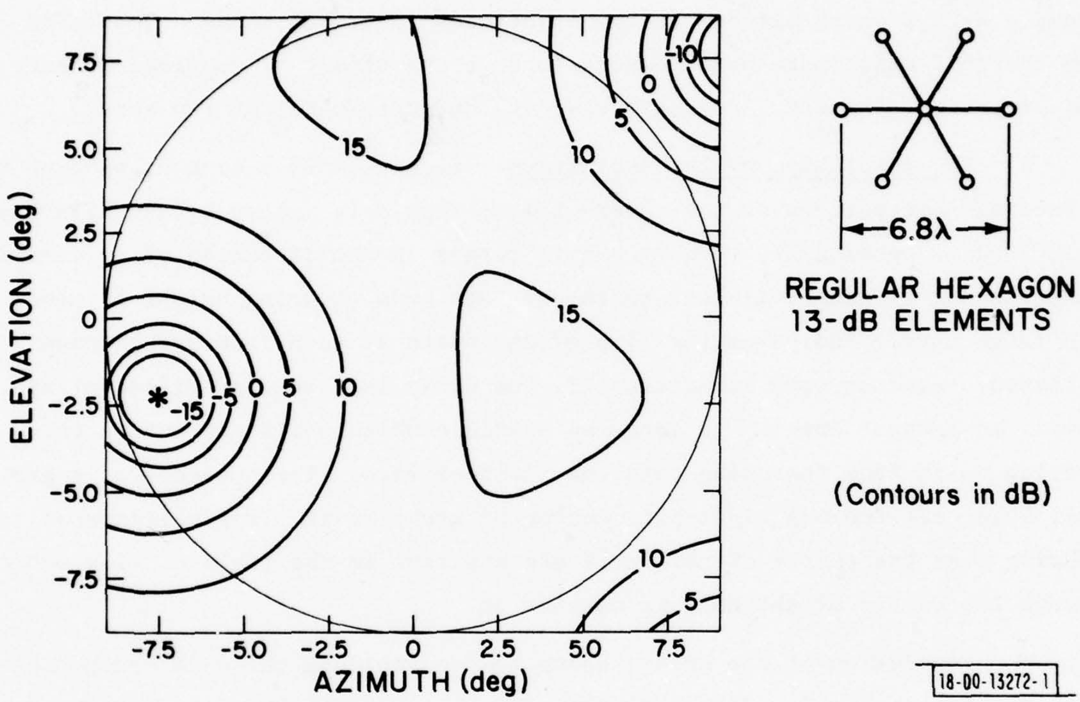

Fig. 14. Directive-gain pattern of a regular hexagonal filled array in the earth-coverage mode with one interference source.

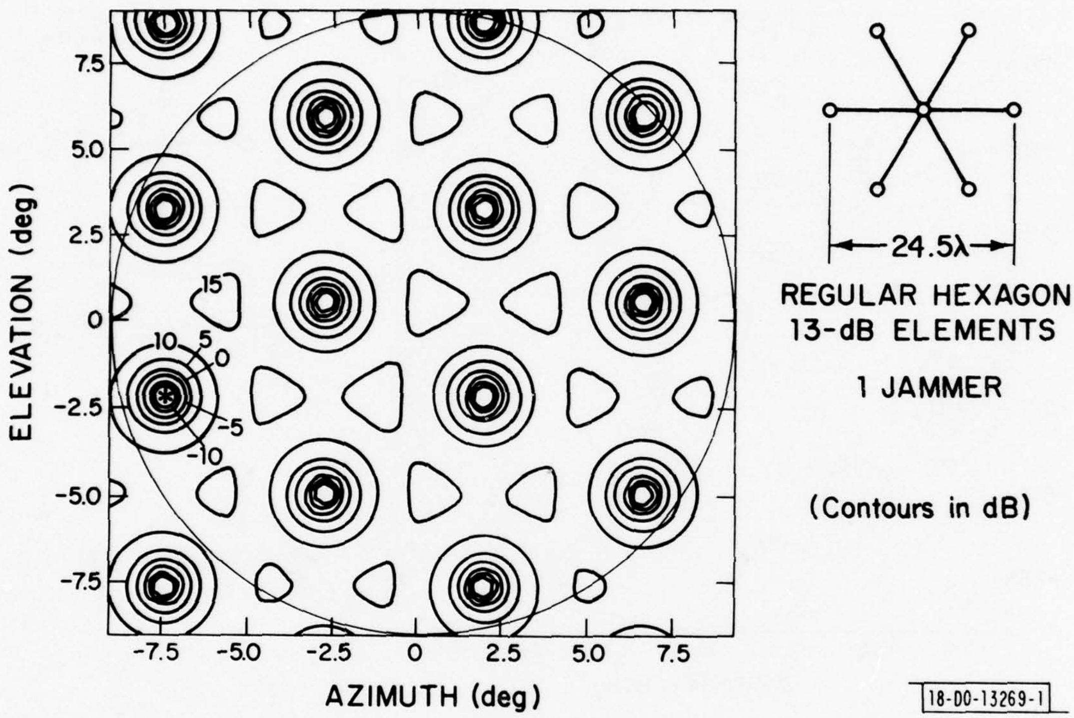

Fig. 15. Directive-gain pattern of a regular hexagonal thinned array in the earth-coverage mode with one interference source.

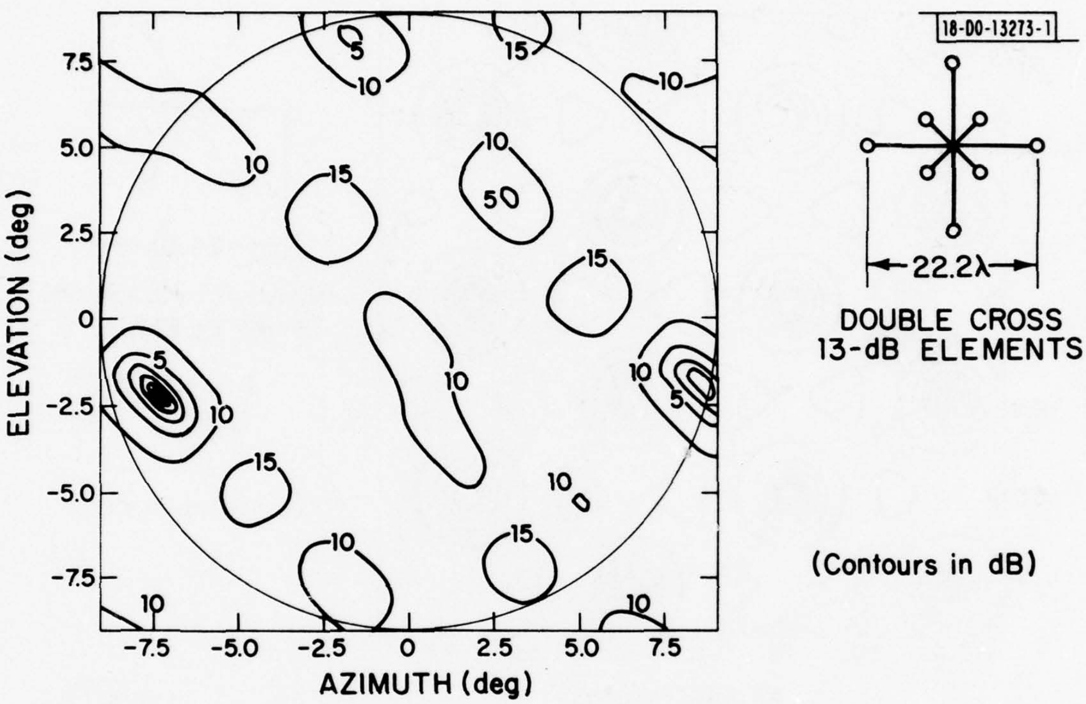

Fig. 16. Directive-gain pattern of a double-cross thinned array in the earth-coverage mode with one interference source.

arrays cancel at the interference source will not be repeated exactly anywhere else in the field of view unless a point exists which is an integral number of lattice-cell widths from the source for both square arrays. There is no such point in Fig. 16, but there is a point, namely (8.6°, -2.2°), which is within half a degree of being two small-lattice-cell widths and three large-lattice-cell diagonals from the source. A quasi grating null, at which cancellation is near perfect, is seen to exist there. Elsewhere, the gain coverage is uneven because of the varying interference between the patterns of each square array, but no other deep nulls occur.

The null on the jammer in Fig. 16 is elliptical rather than round, as it is in Figs. 14 and 15, and so a convenient single measure of the 0-dB resolution is the square root of the product of the principal axes of the ellipse. In this case, it is 1.6°, compared with 1.5° for the slightly larger hexagonal array of Fig. 15 and 5.5° for the small hexagonal array of Fig. 14. Thus the double-cross array of Fig. 16 achieves much the same resolution as the hexagonal array of Fig. 15, and avoids almost completely the grating lobe problem.

An alternative to thinning the small regular hexagonal array of Fig. 14, in order to get greater resolution, is to increase its aperture by adding more elements to obtain the 19-element regular array discussed in Section II. Figure 17 shows what happens then. The resolution is indeed improved, and the gain coverage away from the interference source is much smoother than that of the double-cross array. However, the number of elements (and booms to deploy them) is much larger, and even then the 0 dB resolution is, at 3.4°, more than twice that of the double-cross array. To get the resolution down to 1.5° or so, the aperture would have to be doubled. This would require the addition of two more outer rings of elements, bringing the total to 61, which is at present a prohibitively larger number at UHF.

The foregoing examples have illustrated the merits of thinned arrays for adaptive nulling antennas. The problem now arises of deciding what configuration the thinned array should have. One aspect of the problem is establishing

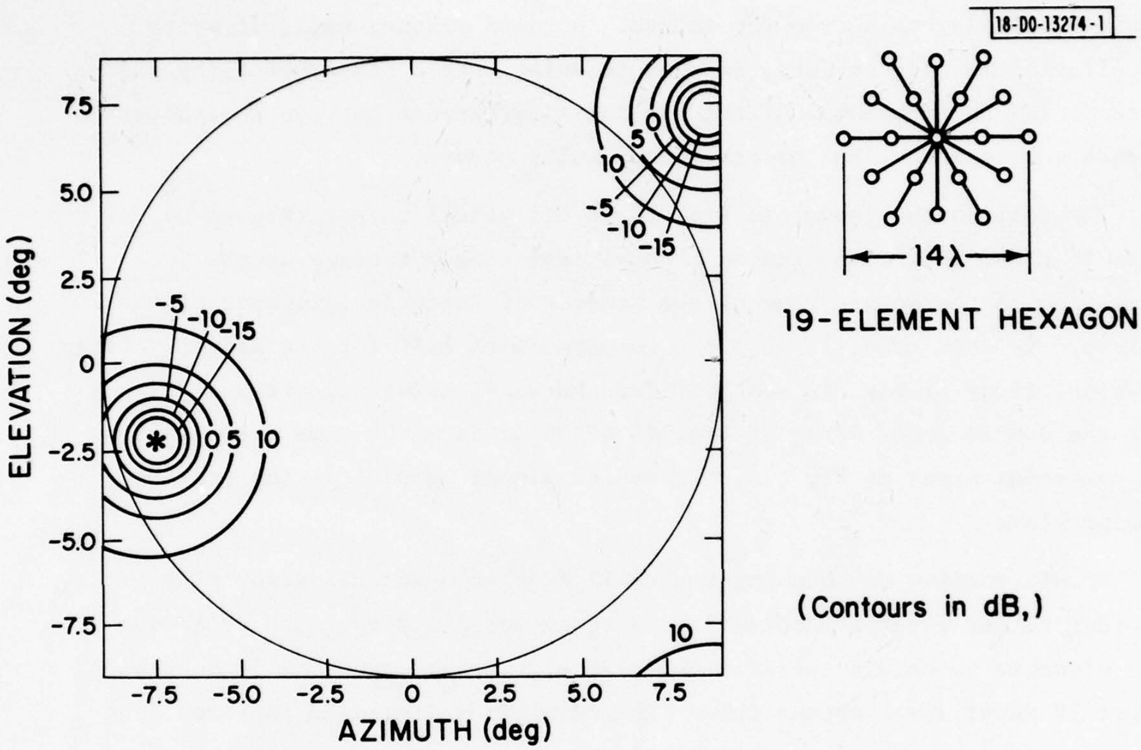

Fig. 17. Directive-gain pattern of a 19-element regular hexagonal filled array in the earth-coverage mode with one interference source.

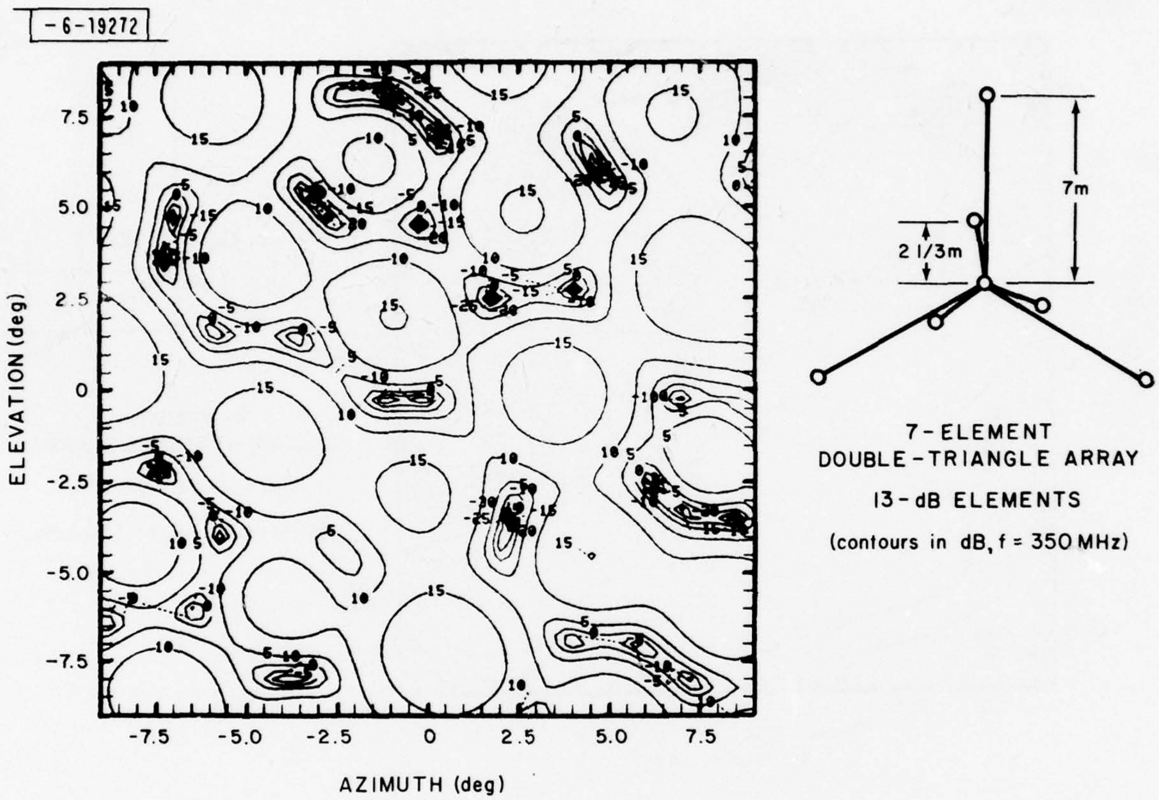

Fig. 18. Directive-gain pattern of a 7-element double-triangle array in the earth-coverage mode with one interference source.

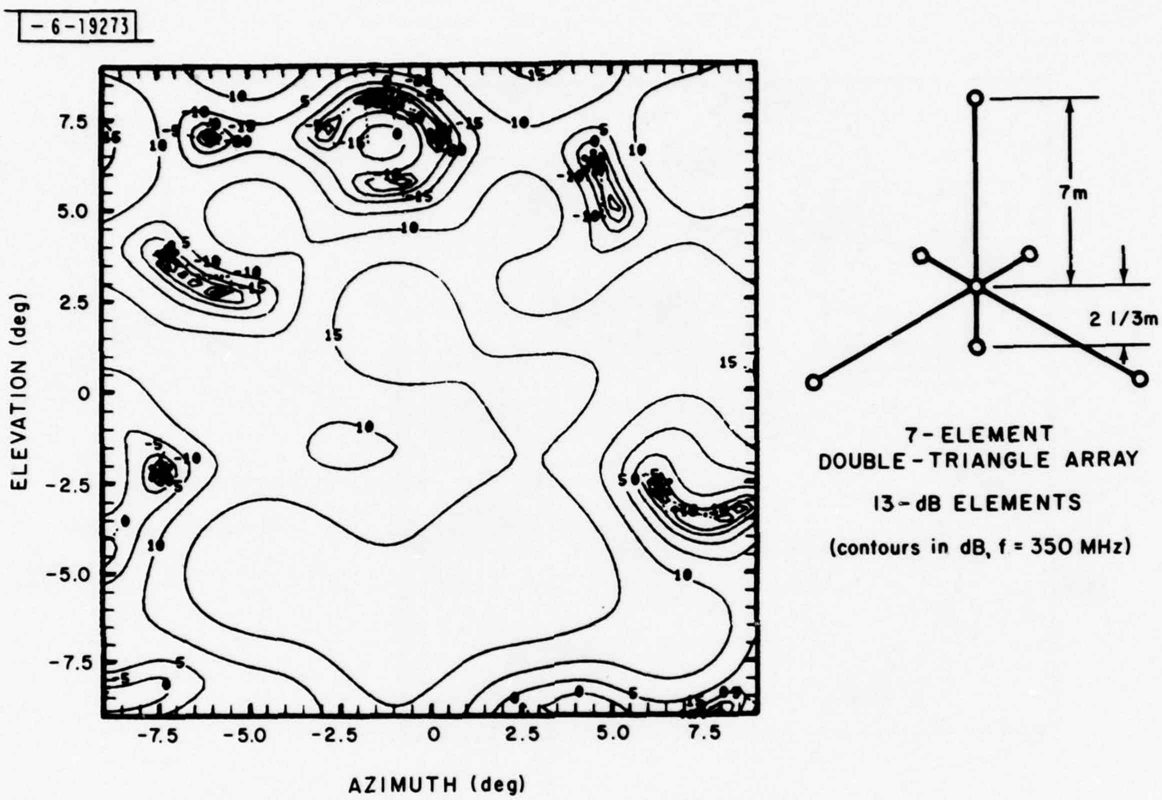

Fig. 19. Directive-gain pattern of a 7-element double-triangle array in the earth-coverage mode with one interference source.

a quantitative measure of the suitability of a configuration, and can be illustrated by reference to Figs. 18 and 19. These are the directive-gain patterns of two slightly different 7-element arrays after adaption to the same scenario of six interference sources. The two patterns are quite different from one another, but are the differences of operational significance? Choosing between the arrays on the basis of contour plots can clearly be a very subjective business.

One way to put the comparison on a more objective basis is to calculate the percentage of the total area for which the gain is greater than a given value, to repeat this for gain values covering the whole range of interest and then to plot the result on a graph showing percentage coverage versus gain.[4] A possible operational requirement might be, for example, that in the presence of three interference sources placed arbitrarily, the array should provide at least 10 dB of directive gain over 70% of the field of view. From the graph, the actual percentage coverage attained by the array can be read off, giving a single number characterizing this aspect of the array performance.

A refinement of the gain coverage presentation which incorporates a measure of the resolution of the array is the construction of separate coverage graphs of the kind described above for subdivisions of the whole disc of the earth. One such region could usefully include just those locations in the field of view falling within say, 0.5° and 1.0° of any interference source. Another could include all locations in the field of view at a distance of greater than 2° from any interference source. A third could be the locations in between these two.

If the locations of the interference sources can vary, then the gain coverage should be recalculated for the various possible source locations. In the limit, when the source locations are arbitrary, a statistical approach is indicated. For this, the source locations would be generated randomly and the mean value of the coverage curve becomes the data of interest, in which the mean is taken over many random source scenarios.

Figure 20 shows the result of such a calculation for the two arrays shown

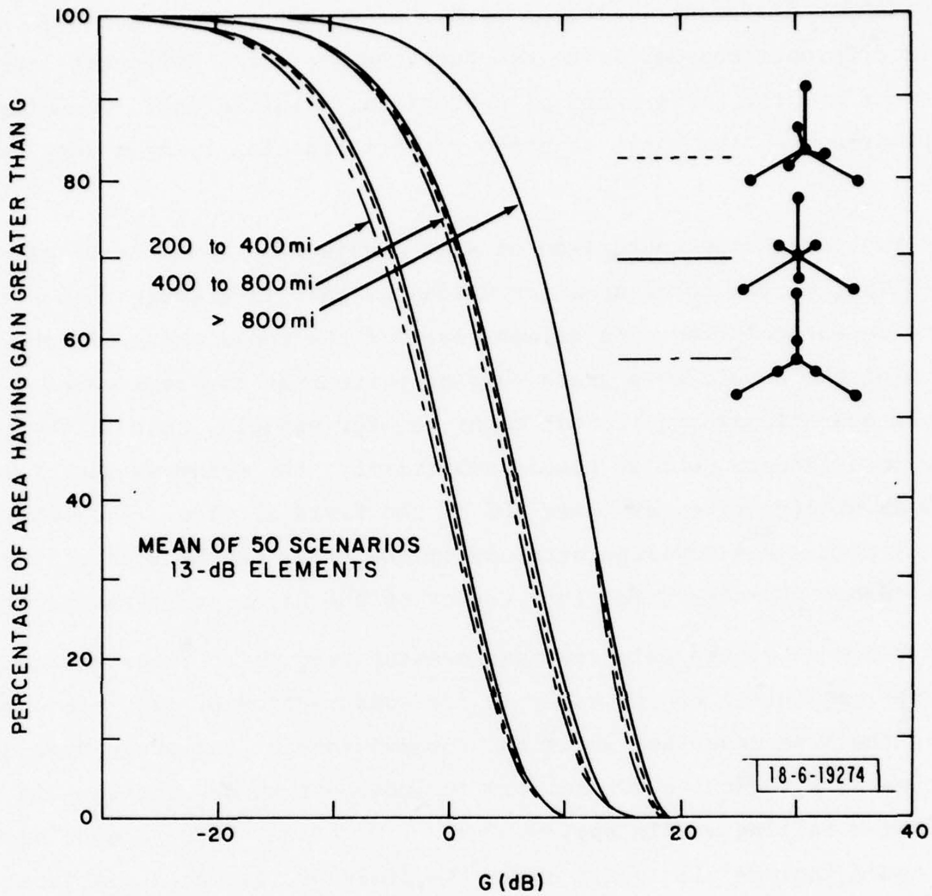

Fig. 20. Average directive-gain coverage curves for the three variations shown of a 7-element double triangle array.

in Figs. 18 and 19 and also for a third which is yet another slight variation of the other two. Figure 20 clearly shows the essentially identical average-coverage performance of the arrays, notwithstanding the profound differences in their contour patterns. (For the coverage curves of Fig. 20, the various coverage regions were defined not in terms of angular distance from the interference sources but of distance in miles on the surface of the earth. The principle is the same, but using miles may be of greater operational significance).

Figures 21 and 22 are the directive-gain coverage curves for three different arrays having essentially the same overall aperture. The first two (the 24.5λ regular hexagon array and the 22.2λ double cross array) have already been introduced via their directive-gain patterns in Figs. 15 and 16. The third is an array which represents a further development of the thinned aperture principle in that it has, as before, a large aperture for good resolution and a double-grid configuration for the elimination of grating nulls but, in addition, has a minimum number of long booms for mechanical simplicity.

The coverage curves in Fig. 21 show that in the outer region (>2° from any interference source), the two irregular thinned arrays (the double cross and the double triangle) provide much better gain uniformity than does the regular thinned array (the 24.5λ hexagon). This is because, as Fig. 15 has shown, this array riddles the region with grating nulls.

Also shown in Fig. 21 is the essentially equal performance of the two irregularly thinned arrays. Thus the 6-element double triangle, needing only three booms for its deployment, is as good an array in this region as the 8-element double cross which needs eight booms (four of medium length and four long ones).

As noted in the Figure (and in Fig. 22), the coverage curves shown were computed using three randomly located interference sources for each of ten scenarios, but the general qualitative nature of the results is the same. The three-source case is presented as an example of the full set. More than five sources would overload the ability of the 6-element double-triangle array to

18-DO-13276-2

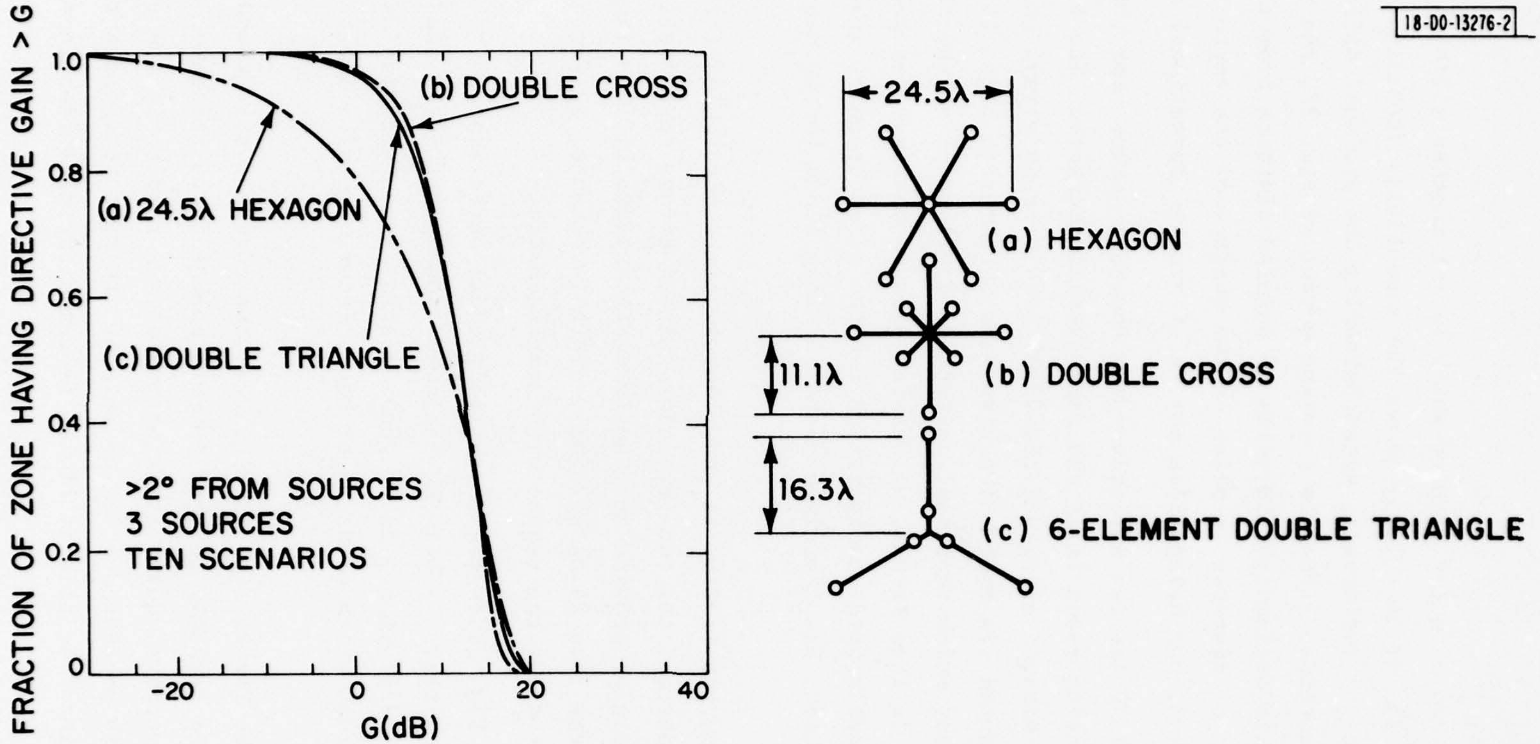

Fig. 21. Average directive-gain coverage curves for three different arrays in the outer (>2°) zone.

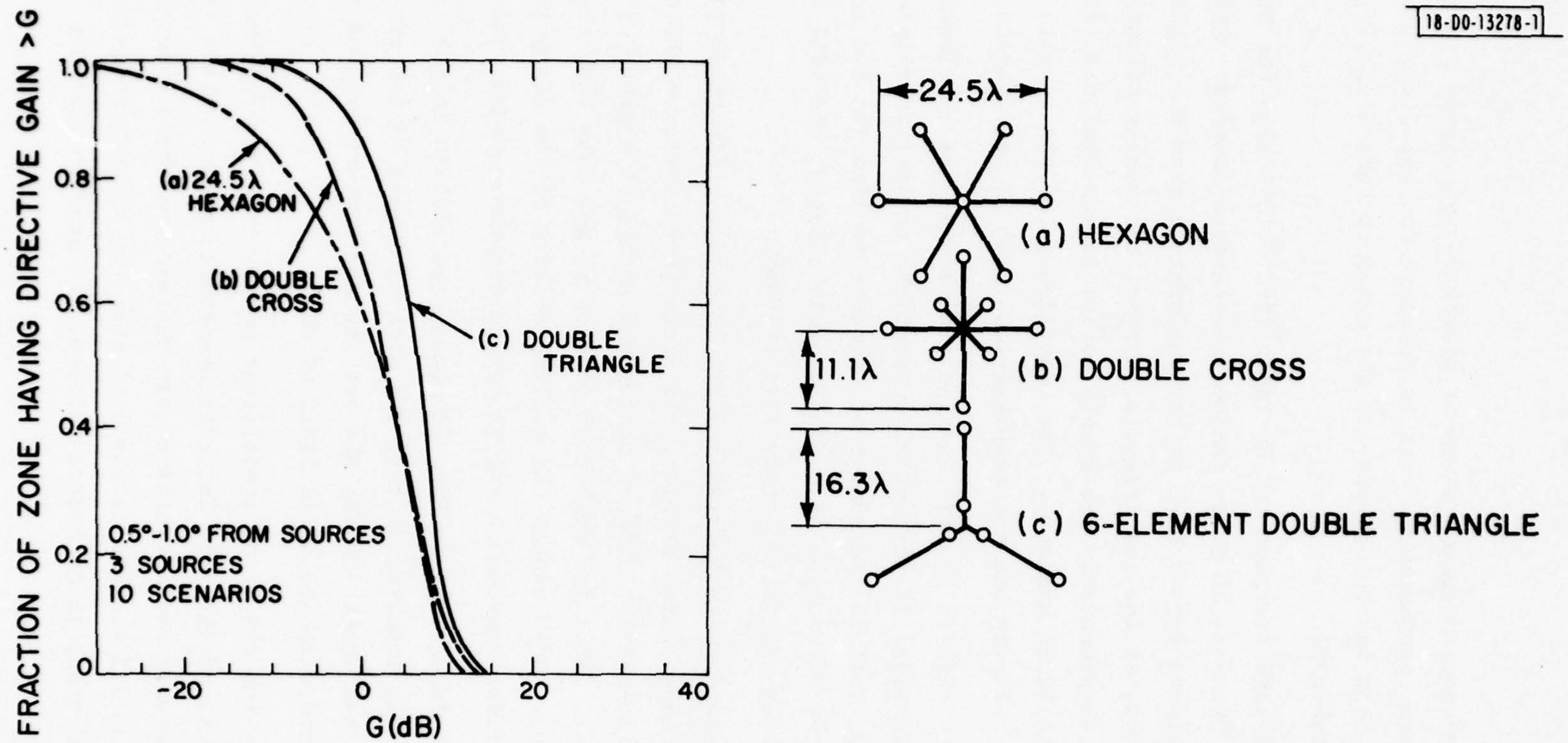

Fig. 22. Average directive-gain coverage curves for three different arrays in the inner (0.5° – 1.0°) zone.

form nulls, in which case coverage curves of directive gain alone are no longer a useful guide to array performance. (It is possible for the directive gain coverage to be good, but for the ability of the array to form usefully deep nulls to be unacceptable.)

Figure 22 shows gain coverage in the inner (0.5°-1.0°) zone for the three arrays in the presence of three random interference sources. Again, the two irregular thinned arrays have better performance than the regular thinned array, but now, of the two irregular arrays, the double triangle has a clear edge. This is presumably due simply to its larger aperture (28.2λ maximum compared with 22.2λ maximum). The significance of the result, however, is that its simpler geometry has not resulted in a loss of performance.

To summarize the results of this Section, therefore, one concludes that the examples given in Figs. 14 through 22 support the general principles stated above, namely, that if the number of elements is limited, the adaptive array will have better resolution if it is severely thinned, and will avoid the grating-null problem if it is irregularly thinned.

C. Grouped Interference Sources and Hybrid Arrays. Figure 20 illustrates the grouped interference source problem. It shows the effect, on the directive gain pattern of a five-element thinned pentagonal array, of a group of seven interference sources. Since the number of sources is not less than the number of array elements, one would expect the nulling ability of the array to be severely impaired if the sources in the group are dispersed widely enough.

For this particular array, as Fig. 23 shows, the ability to null out the sources is markedly impaired in that the directive gain on two of the sources is no less than about -10 dB, and yet the sources are grouped within an area small compared with the whole field of view.

Figure 24 shows the effect on a different array, namely a 7-element double-triangle array, of the same interference-source group. There is a marked difference between this directive gain pattern and the previous one. The directive gain on all sources is now less than -20 dB and the gain coverage away from the source group is much more uniform. It appears that the

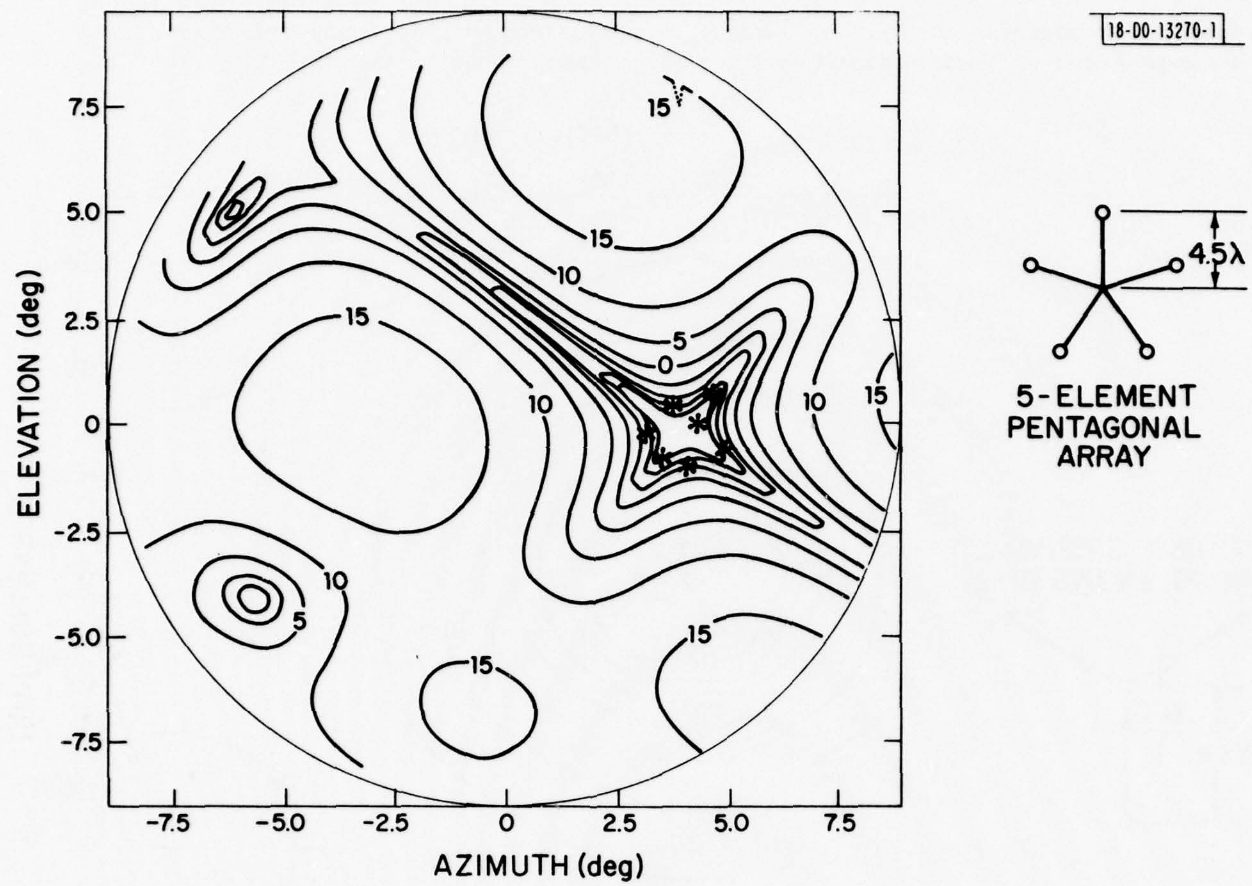

Fig. 23. The directive-gain pattern in the earth-coverage mode of a thinned 5-element array in the presence of a group of seven interference sources.

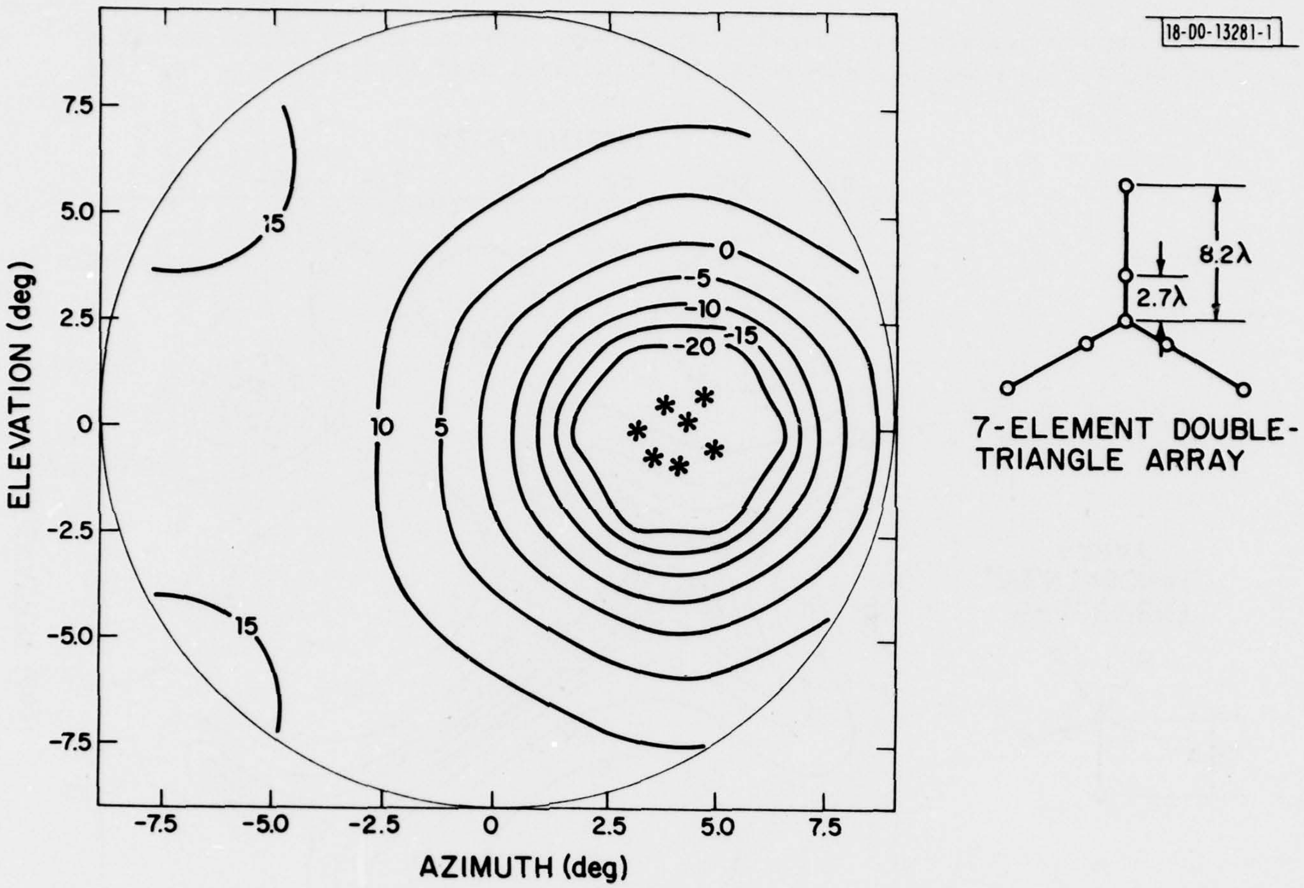

Fig. 24. The directive-gain pattern in the earth-coverage mode of the 7-element double-triangle array in the presence of the same interference-source group used in the preparation of Fig. 23.

interference sources would have to be much more widely dispersed to attack successfully the array of Fig. 24, with its rudimentary filled sub-array, than they would to attack successfully the array of Fig. 23. Figure 25, which compares the interference-suppression coverage curves for the two arrays, confirms this.

The interference-suppression coverage curves in Fig. 25 are calculated in the same way as are the directive-gain coverage curves, except that at each sample location in the zone, the quantity of interest is now the ratio between the directive gain at the location and the average directive gain on the interference sources. The curves are, therefore, a measure of the effectiveness of the nulling array in suppressing the power received from the interference sources.

The curves in Fig. 25 show that the double-triangle array provides at least some 30 dB more jammer interference suppression than the pentagon array, if the jammer interference-source group is no more than 3.6° across. The double-triangle array continues to provide some interference suppression even when the group is 7.2° across, whereas the pentagon array is unable to do so.

On examining the adapted weight vector of the double-triangle array subjected to the grouped jammer attack, one finds that the outer elements are essentially turned off. That is, the adaptive nulling algorithm attempts to reduce the aperture of the array until the resulting null is broad enough to include the whole interference-source group. Only if a smaller sub-aperture exists within the whole aperture can the algorithm do this. The pentagon array has no such sub-aperture and so is vulnerable to the grouped interference sources.

It should be noted that although the physical aperture of the double triangle may be large, the reaction of the nulling algorithm to a grouped-source attack makes the effective aperture much smaller and so degrades the resolution of the array considerably. Thus, although the group in Fig. 24 is unable to disable the whole communication system, it has forced the array

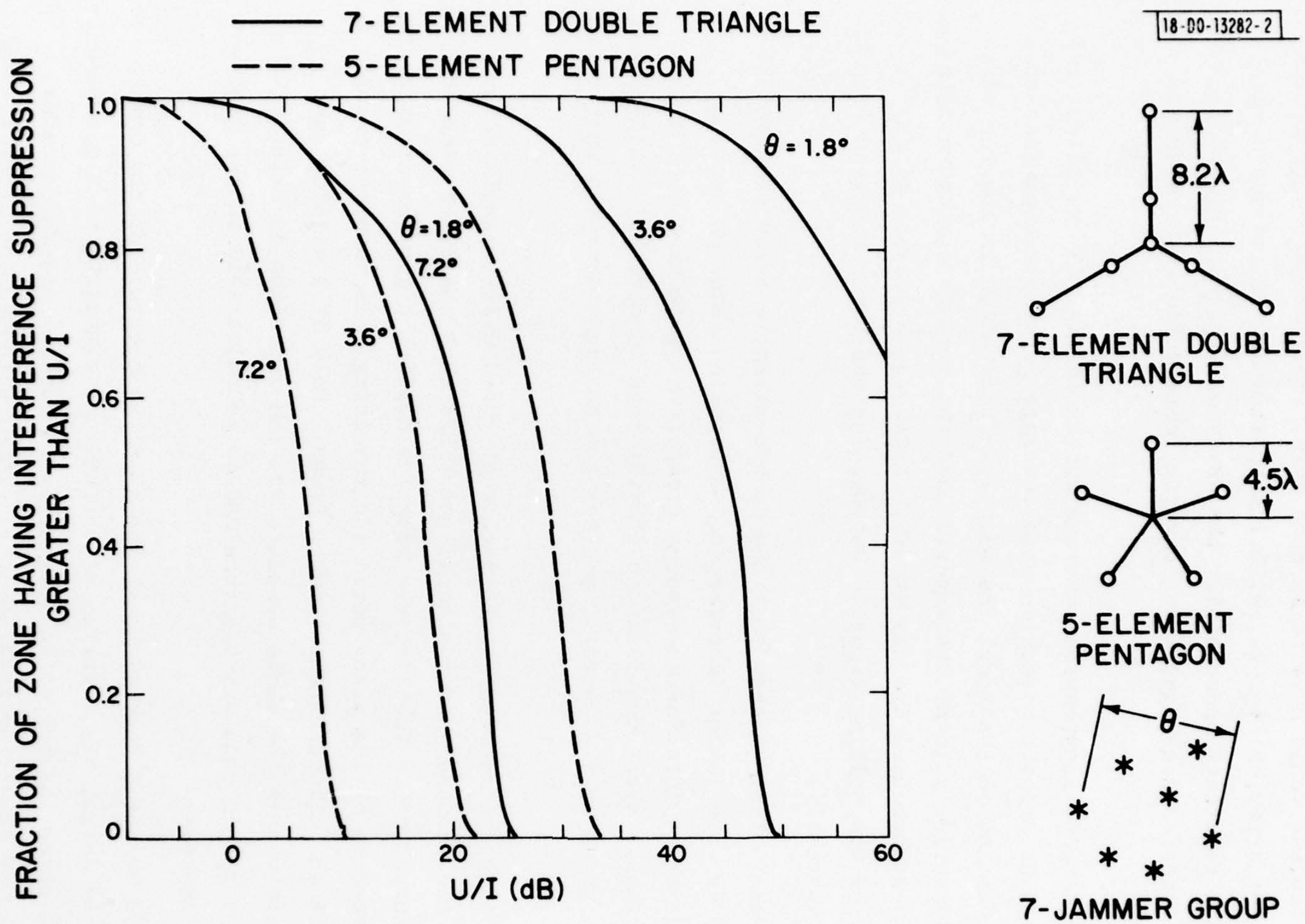

Fig. 25. The interference-rejection coverage curves in the outer (>2°) zone for two arrays attacked by an interference-source group, with group size as a parameter.

to form a broad null with a correspondingly wide transition region surrounding it. In fact, as Fig. 24 shows, the proportion of the field of view having a directive gain of 10 dB or more has been reduced to nearly 50% even though the interference-source group occupies an area some two orders of magnitude smaller than whole field of view.

A question of importance for the subarray concerns its minimum requirements. How few elements are enough and where should they be placed? There is at present no precise answer to the question of placement. The elements clearly should be arrayed in both dimensions of the aperture plane, to give resolution in both dimensions, and since the sub-array alone is active in the presence of a group of sources, the minimum spacing of the elements should be small enough to prevent grating nulls from appearing in the field of view.

The minimum number of elements is determined by the number of "groups" to be nulled. (Here, a scenario in which there is one interference-source group plus, say, three widely dispersed isolated sources, must be regarded as having four source groups. This is because the one real group forces the adaptive array to deactivate all of its elements except those in the sub-array, which must then be able to cope with four effective source locations.) As is the case with the whole array in nulling separate sources, the sub-array needs a minimum of one more element than the number of "groups" it has to deal with. In practice, however, this is not satisfactory. It leads to a minimum of only two elements, for example, if only one group is to be nulled. But such a sub-array has no resolution in one direction. To avoid this problem, at least three elements are required, but even then the result may not be satisfactory when the nulling array is operating in the earth-coverage mode. This is because the standard algorithm, in adapting to a single interference source or a single group, establishes an earth-coverage beam with the earth-coverage element, and then subtracts from it a narrow cancelling beam formed from all the elements together. Unless the phase center of the nulling beam coincides with the phase center of the earth-coverage beam, the interference pattern of the two beams will generate a markedly asymmetric null, in the manner described in Section E below. Achieving phase-center coincidence in a symmetric planar array is not possible with only three elements. A total of at least four elements in the sub-array may be preferred in practice, therefore.

D. Symmetry Questions. An array of N sufficiently separated elements can, with proper adjustment of its N weights, always place nulls on as many as N-1 arbitrarily located interference sources. (The effect of non-zero bandwidth is to fill in the nulls to some extent, but provided the bandwidth is not too great, that is the extent of its effect.) There is no doubt about the intrinsic ability of the array to null N-1 sources. Some uncertainty begins to appear when one asks whether the array can null the N-1 sources and, at the same time, maintain communication with one or more arbitrarily located users. Even more uncertainty is associated with the further question of the effect of array symmetries on the answer to the previous one. At present, completely satisfactory answers to these questions are not available. The following discussion will show that the questions are of importance.

Considering a simple array of just two elements exposed to a single interference source, we find that the array, having only a one-dimensional pattern, can null the source only by generating a line null which is both perpendicular to the line joining the two elements and also passes through the source. This pattern is fully determined and so a user in the line null is also inevitably nulled and a user not in the line null is not nulled. Thus, in this case, a user is also nulled if it is located on a line through the interfering source lying perpendicular to the line joining the two array elements.

In general, for an array of N elements exposed to N-1 interference sources, the directive gain pattern would be expected to be completely determined by the interference sources, if the weights are properly set to form N-1 nulls. Thus, users would be nulled if they lay in the nulls of this pattern, and not otherwise. Since nulls seem invariably to occur as points or lines, however, the fraction of the area of the field of view precisely nulled is mathematically zero. On the other hand, since the null walls are not infinitely steep, there is a non-zero fraction of the field-of-view area within which the users are, for all practical purposes, nulled.

If there are fewer than N-1 interference sources, the extra degrees of freedom not engaged by the sources can be used to form beams favoring particular users. This would seem to suggest that N-I-1 users can always be served, where I is the number of interference sources, but such is not the case as the following example shows.

The array shown in Fig. 26 has six elements but they are arranged in two parallel lines of three. If there are two interference sources lying in a line perpendicular to the parallel lines of the array elements, the condition that the two sources be perfectly nulled leads to the necessity of making the element weights on each parallel line sum to zero. This means that although the array has six elements, the alignment of the elements makes it possible for only two sources to force the array to generate a line null. Thus, if two sources are placed on the line through a distant user which is perpendicular to the two parallel lines of array elements, the sources can in principle null the user from a distance by "aiming" a line null at him. The array shown in Fig. 26 is such that, except for the double lines of three elements discussed above, in no other orientation is it possible to find anything but a minimum of five parallel lines that can be drawn through the elements of the array. This means that to aim a line null having any other orientation than the one shown in Fig. 26 may require five interference sources. This suggests the simple expedient of arranging the elements in such a way that among all the lines connecting each element to one other element, there are no parallel lines.[5] Such an array is the most resistant to line-null aiming.

It should be noted that, at this time, it is not clear whether interference sources can be distributed in such a way as to induce a more general type of null steering. That is to say, even though the array satisfies the "no parallel line" criterion of the last paragraph, and even though the number

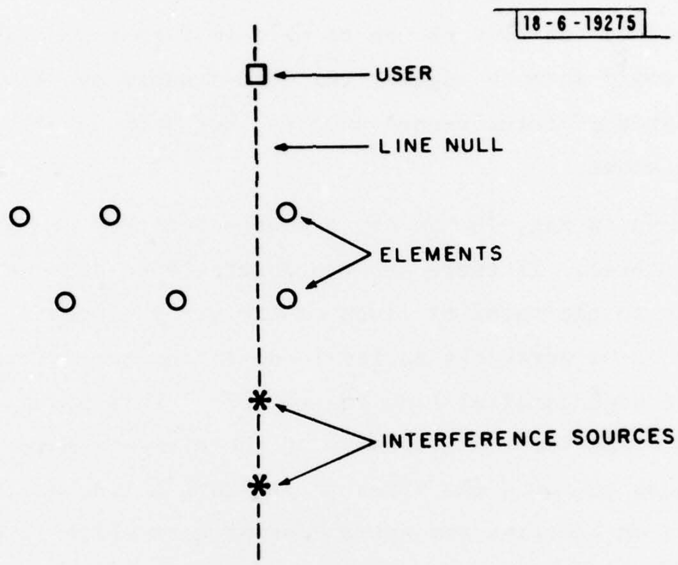

Fig. 26. If the array elements are aligned into J_r parallel lines, J_r interference sources aligned at right angles to the element lines can aim a line null at a user.

of interfering sources is less than the number of antenna elements, it may be possible to locate the sources in such a way as to force the adaptive array to point a null in a direction chosen by this interfering agency but remote from any interfering source. As yet, no theory exists either describing how this might be done or proving that it cannot be done. (On the other hand, if two or more interference sources radiate coherently, the possibility of null steering is known to exist in principle. Whether practical constraints would ever allow such a possibility to be realized is doubtful. In any case, the question of coherent interference sources is not within the scope of this Note.)

E. Resolution and the Choice of Steering Vector. The resolution of a particular array configuration can be shown to be strongly dependent on the phase variation of the quiescent radiation patterns in the vicinity of an interfering source. Hence, for an earth coverage mode of operation, the choice of which element to use as the steering reference arises. To see this, we may envision the nulling process as the formation of two beams; a reference beam combined with an ancillary beam which is weighted to cancel with the reference at the specified point. Clearly, if the phase of the reference beam differs from the phase of the cancelling beam in the area surrounding the interference source, a narrow null will be formed (for example, for a phase difference as small as 6°, only 20 dB cancellation can be obtained) resulting in improved resolution. In order to characterize this effect mathematically, we can consider a one-dimensional pattern characterized by $g(\theta)$, and denote the reference pattern by $g_r(\theta)$ and the cancelling pattern as $g_c(\theta)$. Furthermore, we assume that a null is to be formed at $\theta = 0$. Then

$$g(\theta) = g_r(\theta) - \alpha g_c(\theta) \quad , \tag{11}$$

where α is given by $\alpha = g_r(0)/g_c(0)$. In the vicinity of the null, we can expand $g(\theta)$ in the form

$$g(\theta) = g(0) + g'(0)\theta + g''(0)\,\theta^2/2 + \ldots \quad . \tag{12}$$

Clearly, $g(0) = 0$, so that $g(\theta)$ can either be linear or quadratic as we move away from the null. The former leads, in general, to better resolution than the latter. Denoting the phase of $g_r(\theta)$ as $\phi_r(\theta)$ and of $g_c(\theta)$ by $\phi_c(\theta)$, and assuming for now that the amplitude of each beam varies slowly close to $\theta=0$, we can write

$$g(\theta) \sim j\left(\frac{d\theta_r}{d\theta} - \frac{d\phi_c}{d\theta}\right)\theta + O(\theta^2) \quad . \tag{15}$$

Hence, the rate of change of the phase difference between the beams governs the nulling resolution. Clearly, for a symmetric type of array with a center-of-phase element reference, $\phi_r=\phi_c$ and a quadratic null results. If an element other than a center-of-phase element is chosen for reference (e.g., the 5-element pentagon, or an outer element of the double triangle), then $\theta_r\neq0$ and better nulling resolution results.

This effect in shown in Fig. 27 for the seven-element double-triangle array. The two sets of gain coverage curves were obtained in the adaptive earth-coverage mode using either the center element or an arm-end element as the quiescent earth-coverage element. The higher resolution of the "arm-end" adapted pattern is clearly evident. In fact, the gain in the inner zone (200-400 miles from the interference source) is higher on average by some 7 dB when the earth-coverage element is chosen to be an arm-end element than when it is the center element.

This higher resolution is due solely to the phase-slope effect described above. When the earth-coverage element is at the center of the array, the null is quadratic, because there is no difference in phase slope between the reference (earth-coverage) beam and the cancelling beam. When the earth-coverage element is at an arm end, the null is linear because the phase-slope, or interferometer, effect dominates the quadratic, or beam shape effect, giving a higher resolution.

Also shown in Fig. 27 is the shape of the 0-dB gain contour around the interference source, for the two choices of earth-coverage element. The much reduced enclosed area of the "arm-end" case implies a much higher resolution. It should be noted, however, that the resolution has improved only along one

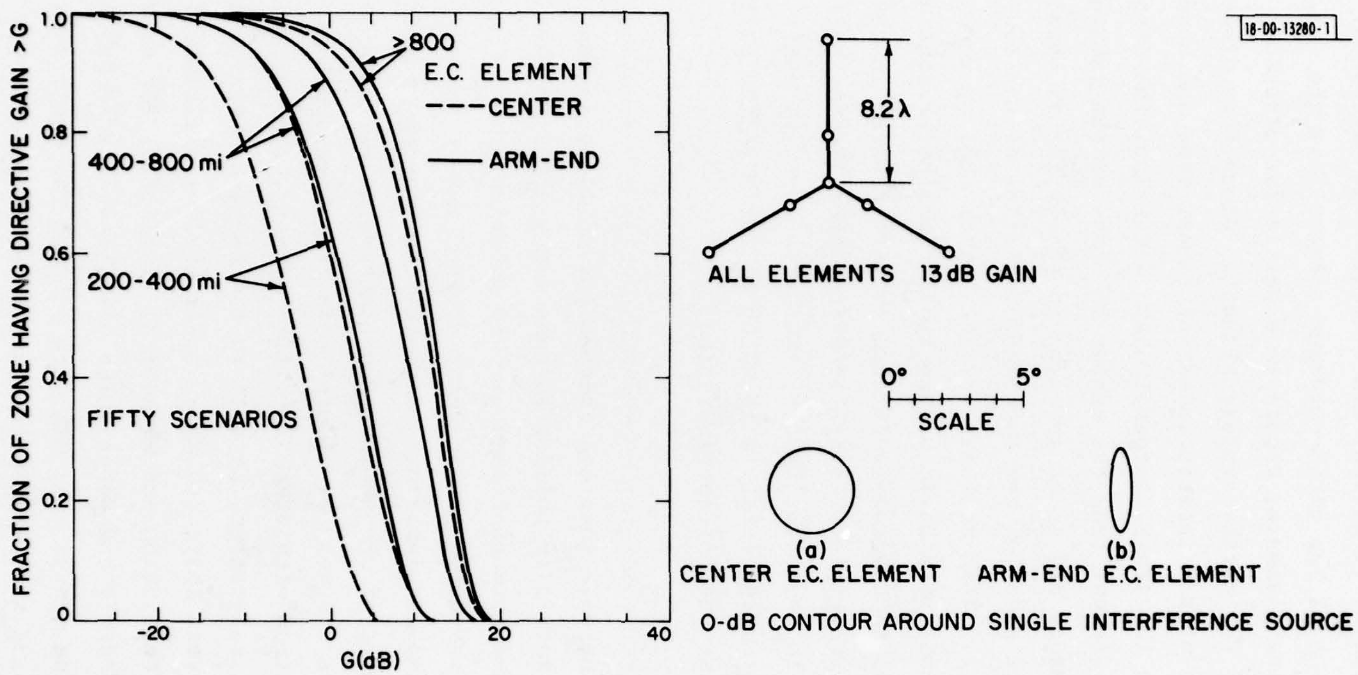

Fig. 27. Using an outer element as the earth-coverage element, rather than the center element, improves resolution. The gain-coverage curves, and the null size, both reflect this improvement.

axis. In the perpendicular direction, the resolution is unaltered. This is because the displacement of the earth-coverage element from the center of phase of the remaining nulling elements, occurs in a particular direction no matter what choice is made of the earth-coverage element. Along this direction, the resulting null will be of the interferometer or linear type and hence be of higher resolution. In the other, perpendicular, direction, the displacement of the earth-coverage element from the center of phase of the remaining elements is still effectively zero, and so no increase in resolution is obtained. A similar argument can be made for the amplitude variation of the two interacting patterns about the null. This accounts for the better nulling resolution obtained when $\underline{V}$ corresponds to a maximum directivity beam pointed to a user, rather than the flat earth-coverage reference pattern treated in the simulations above. (Note: if the array elements are identical, the element pattern factors out so that, relative to the array factor, the earth coverage pattern is "flat.") Thus, still another parameter exists with which to optimize the nulling performance of a particular antenna configuration.

V. SUMMARY AND CONCLUSIONS

To be sure of being able to place independent nulls on as many as N-1 interference sources, a satellite nulling antenna array needs to have at least N independently weighted antenna elements. The question of where these elements should be placed relative to one another has no easy answer because of the difficulty, on the one hand, of defining a satisfactory measure of system performance, and, on the other, of the number of parameters to be taken into consideration. Some of these are weight, element gain, required depth of null, ease of deployment, interaction with other satellite systems, type of user coverage desired, and component tolerances, as well as the numbers defining the location of the elements. However, there are some rather obvious desirable properties of the array, such as resolution and mechanical simplicity, for example, which can be dealt with separately and about which some general statements can be made. This provides the system engineer with some of the basic data he needs to do his job of defining the optimum combination of properties for his particular application.

The simplest configuration is that in which the antenna elements are located at the nodes of a regular plane lattice. As in conventional phased arrays, the spacing between the elements needs to be of the order of a half wavelength if grating lobes are to be avoided completely. However, for the uplink of a synchronous satellite, the elements of the receiving array can be as much as 3 or more wavelengths apart, because our concern with grating lobes then becomes only that of keeping them off the narrow field of view that the disc of the earth presents from synchronous altitude. Such a regular array, having no grating lobes in the field of view, can be referred to as a filled array. It provides good control of gain distribution, it has the same number of degrees of freedom as there are beams of maximum-gain that can be fitted into the field of view, and it can provide some resistance to interference from sources equal to or greater in number than the number of degrees of freedom, provided the sources are not distributed uniformly over the field of view.

However, in principle N elements can place nulls on N-1 interfering sources no matter where the elements are located, although in practice the elements should not be too close to one another. Thus, by removing some elements from the filled array and relocating them at other more widely spaced lattice points, we obtain an array that still can null N-1 interference sources but, in addition, has greater resolution on account of its larger aperture. Such an array can usefully be referred to as a thinned array, because many of the lattice points within the overall array aperture are not occupied by array elements. By maintaining the original lattice spacing for some elements, but at the same time greatly increasing the spacing between other elements, one can avoid grating lobe problems and yet achieve a greatly improved resolution. However, since the number of degrees of freedom of the field of view is now much greater than the number of antenna elements, one no longer has tight control of the overall gain coverage.

The actual element locations are determined by a tradeoff between resolution, weight, gain coverage away from the nulls and ease of deployment. It appears, for example, that an overall aperture need be defined by only three elements, and still achieve the resolution implied by that aperture. Only three long booms are needed to deploy these elements.

Quantitative assessment of the performance of the array is most conveniently carried out using coverage curves of directive-gain or interference suppression in which the fraction of the area of the field of view, over which the adapted directive gain or interference suppression of the array exceeds a certain value, is plotted as a function of that directive gain or interference suppression value. This can be repeated for different locations, and numbers, of interference sources, and for different array configurations and nulling algorithms. Comparison between the results is then directly quantitative rather then subjective, as it would be were contour plots alone to be used.

There is a particular vulnerability of the thinned array to grouped interference sources. Since the half-power beamwidth of a thinned array can be much less than that of a filled array with the same number of elements, it is possible to place N or more interference sources within a region much smaller in area than the whole field of view, and still completely overcome the resistance of the array to interference. One can deal with this problem to some extent by retaining within the whole thinned array, a smaller filled sub-array. Such a hybrid array is much more resistant to grouped interference sources than a simple thinned array, but it still suffers from a loss of resolution in the presence of the grouped interference sources. A filled array of the same overall aperture can resist the grouped sources and still retain its high resolution, but typically it would have an order of magnitude greater number of elements.

Another consideration in the configuration of both filled and thinned arrays is "symmetry vulnerability". An array with its elements placed along a very few straight lines which are parallel to one another is still able to place nulls on as many as N-1 interference sources, but far fewer interference sources can force the adaptive array to generate a line null. Proper placing of the interference sources can therefore induce the array to place a null on a particular user, provided only that the user location and the orientation of the array are known to the interfering agency. It would seem to be advantageous, therefore, to configure the elements in such a way that a straight line through any pair of elements is not parallel to any other such line. However more work on this question is needed.

REFERENCES

1. J. T. Mayhan, "Adaptive Nulling with Multiple Beam Antennas", Technical Note 1976-18, M.I.T. Lincoln Laboratory (30 September 1976), DDC AD-A034652/8.

2. W. F. Gabriel, "An Introduction to Adaptive Arrays", Proc. IEEE 64, (1976), pp. 239-271.

3. D. H. Martin, "Communication Satellites 1958-1980", SAMSO Report TR-77-76, Aerospace Corporation (1 February 1977), p. 197.

4. L. J. Ricardi, "A Summary of Methods for Producing Nulls in an Antenna Radiation Pattern", Technical Note 1976-38, M.I.T. Lincoln Laboratory (2 September 1976), DDC AD-A032340/2.

5. A. F. Culmone (private communication).

UNCLASSIFIED

SECURITY CLASSIFICATION OF THIS PAGE (When Data Entered)

14 TN-1978-5

19

REPORT DOCUMENTATION PAGE

READ INSTRUCTIONS BEFORE COMPLETING FORM

1. REPORT NUMBER: 18 ESD-TR-78-288	2. GOVT ACCESSION NO.
3. RECIPIENT'S CATALOG NUMBER	
4. TITLE (and Subtitle): 6 Configuration Tradeoffs for Satellite Nulling Arrays.	5. TYPE OF REPORT & PERIOD COVERED: 9 Technical Note
	6. PERFORMING ORG. REPORT NUMBER: Technical Note 1978-5
7. AUTHOR(s): 10 Michael L. Burrows ~~and~~ Joseph T. Mayhan	8. CONTRACT OR GRANT NUMBER(s): 15 F19628-78-C-0002
9. PERFORMING ORGANIZATION NAME AND ADDRESS: Lincoln Laboratory, M.I.T., P.O. Box 73, Lexington, MA 02173	10. PROGRAM ELEMENT, PROJECT, TASK AREA & WORK UNIT NUMBERS: Program Element Nos. 33126K and 63431F, 16 Project No. 2029
11. CONTROLLING OFFICE NAME AND ADDRESS: Air Force Systems Command, USAF, Andrews AFB, Washington, DC 20331; Defense Communications Agency, 8th Street & So. Courthouse Road, Arlington, VA 22204	12. REPORT DATE: 11 21 November 1978
	13. NUMBER OF PAGES: 68 (12 66p)
14. MONITORING AGENCY NAME & ADDRESS (if different from Controlling Office): Electronic Systems Division, Hanscom AFB, Bedford, MA 01731	15. SECURITY CLASS. (of this report): Unclassified
	15a. DECLASSIFICATION DOWNGRADING SCHEDULE

16. DISTRIBUTION STATEMENT (of this Report)

Approved for public release; distribution unlimited.

17. DISTRIBUTION STATEMENT (of the abstract entered in Block 20, if different from Report)

18. SUPPLEMENTARY NOTES

None

19. KEY WORDS (Continue on reverse side if necessary and identify by block number)

adaptive nulling	uplink	communications
coverage	array antenna	vulnerability
multiple beam antenna	interference	

20. ABSTRACT (Continue on reverse side if necessary and identify by block number)

This paper reviews many of the factors to be considered in deciding upon the relative locations of the elements of an adaptive nulling uplink array antenna on a communications satellite. Discussed are the implications of the limited field of view, the desired resolution, the required coverage away from the null, the weight of the array and its ease of deployment and the resistance to grouped interference sources. Filled arrays, having a performance essentially identical to that of a multiple beam antenna, are described, followed by thinned arrays with their increased resolution but greater vulnerability to grouped interference sources, and hybrid arrays which combine the two array types in an attempt to reduce this vulnerability.

207 650

JOB